

# Accepted Manuscript

Synthesis and evaluation of 7,8-dehydrorutaecarpine derivatives as potential multifunctional agents for the treatment of Alzheimer,s disease

Yan He, Pei-Fen Yao, Shuo-bin Chen, Zhi-hong Huang, Shi-Liang Huang, Jia-Heng Tan, Ding Li, Lian-Quan Gu, Zhi-Shu Huang



PII: S0223-5234(13)00108-6

DOI: [10.1016/j.ejmech.2013.02.014](https://doi.org/10.1016/j.ejmech.2013.02.014)

Reference: EJMECH 6004

To appear in: *European Journal of Medicinal Chemistry*

Received Date: 14 December 2012

Revised Date: 31 January 2013

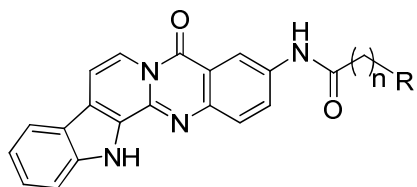
Accepted Date: 13 February 2013

Please cite this article as: Y. He, P.-F. Yao, S.-b. Chen, Z.-h. Huang, S.-L. Huang, J.-H. Tan, D. Li, L.-Q. Gu, Z.-S. Huang, Synthesis and evaluation of 7,8-dehydrorutaecarpine derivatives as potential multifunctional agents for the treatment of Alzheimer,s disease, *European Journal of Medicinal Chemistry* (2013), doi: 10.1016/j.ejmech.2013.02.014.

This is a PDF file of an unedited manuscript that has been accepted for publication. As a service to our customers we are providing this early version of the manuscript. The manuscript will undergo copyediting, typesetting, and review of the resulting proof before it is published in its final form. Please note that during the production process errors may be discovered which could affect the content, and all legal disclaimers that apply to the journal pertain.

## Synthesis and evaluation of 7,8-dehydrorutaecarpine derivatives as potential multifunctional agents for the treatment of Alzheimer's disease

Yan He, Pei-Fen Yao, Shuo-bin Chen, Zhi-hong Huang, Shi-Liang Huang, Jia-Heng Tan, Ding Li, Lian-Quan Gu, Zhi-Shu Huang\*



Twenty seven new 3-aminoalkanoamido-substituted 7,8-dehydrorutaecarpine derivatives were synthesized as multifunctional anti-Alzheimer agents, these compounds showed activities of cholinesterase inhibition, self and AChE-induced A $\beta$  aggregation inhibition, antioxidation, and metal chelation.

**Title Page****Synthesis and evaluation of 7,8-dehydrorutaecarpine derivatives as potential multifunctional agents for the treatment of Alzheimer's disease**

Yan He, Pei-Fen Yao, Shuo-bin Chen, Zhi-hong Huang, Shi-Liang Huang, Jia-Heng Tan, Ding Li, Lian-Quan Gu, Zhi-Shu Huang\*

*School of Pharmaceutical Sciences, Sun Yat-sen University, Guangzhou 510006, People's Republic of China*

\*To whom correspondence should be addressed. Tel.: 8620-39949056, Fax.: 8620-39943056, e-mail: ceshzs@mail.sysu.edu.cn.

**Abstract**

A series of 7,8-dehydrorutaecarpine derivatives were synthesized and characterized as potential multifunctional agents for treatment of Alzheimer's disease (AD). All of these synthetic compounds showed high acetylcholinesterase (AChE) inhibitory activity with  $IC_{50}$  values ranged from 0.60 to 196.7 nM, and good selectivity for AChE over butyrylcholinesterase (BuChE) (125- to 3225-fold). A Lineweaver-Burk plot and molecular modeling study indicated these compounds could bind to both catalytic active site and the peripheral anionic site of AChE. Besides, compounds showed higher activity of inhibiting AChE-induced amyloid-beta ( $A\beta$ ) aggregation than curcumin, higher anti-oxidative activity than Trolox, and could also be good metal chelators. Considering their low cytotoxicity, our results indicated that these derivatives provide good templates for developing new multifunctional agents for AD treatment.

**Keywords:**

7,8-dehydrorutaecarpine derivatives  
Alzheimer's disease  
Acetylcholinesterase  
 $A\beta$  aggregation  
Antioxidant  
Metal-chelating

**Abbreviations:**

AD: Alzheimer's disease  
AChE: acetylcholinesterase  
BuChE: butyrylcholinesterases  
 $A\beta$ : amyloid  $\beta$ -peptide  
PAS: peripheral anionic site  
CAS: catalytic active site  
MTT: methyl thiazolyl tetrazolium  
ORAC: oxygen radical absorbance capacity  
ThT: thioflavin T

## 1. Introduction

Alzheimer's disease (AD) is clinically characterized by a progressive and irreversible cognitive impairments and memory loss [1]. The treatment for AD remains a challenge for pharmaceutical scientist. Although the pathogenesis of AD is not completely known, several factors, such as cholinergic hypothesis, amyloid-beta ( $A\beta$ ) aggregation, tau hyperphosphorylation, and oxidative stress have been considered to play definitive roles in its etiology [2]. The treatment with acetylcholinesterase inhibitors (AChEIs), such as donepezil, rivastigmine, and galantamine, based on so-called cholinergic hypothesis, has been used as therapeutic approach for AD treatment [3]. However, the functions of butyrylcholinesterase (BuChE), another type of cholinesterase, which is mainly abundant outside human brain, are still unclear. Several studies have suggested that inhibition of BuChE may contribute to the peripheral side effects of cholinesterase inhibitors [4], like the dual AChE and BuChE inhibitors tacrine, which showed serious hepatotoxicity and other side effects [5]. In addition, it has been recently reported that in *vivo* BuChE activity is not increased in Alzheimer's disease synapses of patients [6]. Therefore, it may be a good approach to develop specific AChE inhibitors for the treatment of AD, with expectation for their fewer side effects.

The progressive aggregation and deposition of  $A\beta$ , one of the major neuropathological features in AD patients, is considered to be crucial to the pathology [7]. In particular,  $A\beta_{1-42}$  is the predominant form in amyloid plaques, revealing lower solubility and stronger neuronal toxicity than  $A\beta_{1-40}$  [8]. Preventing the formation and aggregation of  $A\beta$  is a potential method for AD treatment [9]. In order to achieve this purpose, several series of inhibitors were being pursued, such as curcumin, Congo-red, benzofuran, acridone and rifampicin derivatives or analogues [10, 11], to disrupt the process of  $A\beta$  fibrillization. Recent molecular dynamics simulation studies revealed that aromatic residues of  $A\beta$  played a crucial role in the formation and

stabilization of polymeric structures [12-14]. Several polyphenols and other small aromatic molecules were displayed to inhibit the amyloid aggregation [15, 16]. Besides, the strategy of designing peptide-based inhibitors which can interrupt the  $\beta$ -sheet structure of the amyloid core or can form complexes with the helical elements in the primary structure of the amyloidogenic peptide to prevent the formation of amyloid structures is effective [17-19]. On the other hand, recent studies have reported the ability of purified AChE to promote the assembly of A $\beta$  peptide into amyloid fibril, which was so-called AChE-induced A $\beta$  aggregation. There is evidence that AChE can bind to the A $\beta$  non-amyloidogenic form, forming with them stable complexes by means of a protein-protein interaction, enhancing the aggregation of A $\beta$  fragments and accelerating the conformational transition into amyloid fibrils and senile plaques [20]. The aggregation-promoting action seems to be associated with a structural domain, located close to the entrance of the AChE active-site gorge, perhaps overlapping the peripheral anionic site (PAS) of AChE other than the active center [21, 22]. Thus, inhibiting the PAS of AChE can affect the AChE-induced A $\beta$  aggregation [21-23]. On this premise, novel classes of AChE inhibitors targeting PAS have emerged as promising anti-Alzheimer drug candidates [24].

During aging, the progressive damage of the endogenous antioxidant protection system is another obvious phenomenon in AD. Moreover, increasing evidence supports the significant impact of oxidative stress in the pathogenesis and progression of AD [25, 26]. Recent studies have indicated that oxidative damage could promote the appearance of amyloid plaques and neurofibrillar tangles in AD [27]. Thus, drugs that aimed at clearing or preventing the formation of the free radicals could be useful for AD treatment. It has been suggested redox-active metal ions like Cu<sup>2+</sup> and Fe<sup>2+</sup> might contribute to the production of reactive oxygen species (ROS) and oxidative stress [28]. Therefore, metal chelators, such as desferrioxamine [29], clioquinol (CQ) [30], and 8-hydroxyquinoline derivative (PBT2) [31] have been proposed as potential therapeutic

substances for the treatment of AD [32].

The development of multifunctional agents with two or more correlative biological activities, corresponding with the multi-factors causing AD, has drawn most attention for their important advance in the treatment of AD [33], while it remains a difficult task. Selecting a promising lead compound becomes the key point to explore potential multifunctional drugs. We have previously studied a series of rutaecarpine derivatives as selective AChE inhibitors, and found that the compounds with 7,8-dehydrorutaecarpine (**DHRu**, Fig.1) moiety had better potency than that of derivatives with rutaecarpine (**Ru**, Fig.1) moiety [34]. Moreover, it has been reported that carbazole derivatives have the capacity of inhibiting A $\beta$  aggregation [35] with free-radical-scavenging effect [36]. Thus, we are interested in the development of novel 7,8-dehydrorutaecarpine derivatives as potential multifunctional agents for the treatment of Alzheimer's disease. In the present study, a series of new 3-aminoalkanamido-substituted 7,8-dehydrorutaecarpine derivatives (Fig.1) were designed, synthesized, and evaluated for their biological activity, including inhibition of cholinesterase, inhibitory effects on self and AChE-induced A $\beta$  aggregation, anti-oxidative activity, and metal chelating property.

## 2. Chemistry

The synthetic pathway for 3-aminoalkanamido-substituted 7,8-dehydrorutaecarpine derivatives **9a-9l**, **10a-10n**, **11a**, **11c**, **11f** and **11l** is shown in Scheme 1. Compounds **9e**, **9f** and **9g** have been reported in our previous work [34]. The synthetic methodology for the key intermediate 3-amino-rutaecarpine (**6**) followed the Bergman pathway with minor modification [37], as shown in Scheme 2. Firstly, reaction of the nitro isatoic anhydride with tryptamine under reflux for 2h in pyridine containing trifluoroacetic anhydride gave **3**

in 50% yields. Then, compound **3** was cyclized to **4** in HCl-AcOH conditions under reflux for 1h in 95% overall yield. The compound **4** was hydrogenated in the catalysis of 10% Pd/C, yielding the compound **5**. Lastly, the treatment of **5** with alcoholic KOH eliminated the fluoroform group, providing the compound **6** in 99% yields.

The preparation for intermediates **7a-7c** was accomplished by the acylation of **6** with appropriate acyl chloride, following a previously reported procedure [34]. The treatment of compounds **7a-7c** with DDQ in dioxane under reflux for 12h gave the dehydrogenated **8a-8c**. Finally, the lead compounds **9a-9k**, **10a-10k**, **11a**, **11c** and **11f** were obtained from **8a-8c** in the presence of appropriate amines under reflux for 8h. The preparation for intermediates **12a-12c** was accomplished by the condensation reaction of **6** with appropriate aromatic acid, followed by the dehydrogenation with DDQ, giving the lead compounds **9l**, **10l** and **11l**. In addition, the methylation of compounds **10d** and **10f** with iodomethane in thiocyclopentane produced the lead compounds **10m** and **10n** (Scheme 1). The structures of the lead compounds were validated by using  $^1\text{H}$  NMR,  $^{13}\text{C}$  NMR, and HRMS, and their purities were determined to be above 95% by using HPLC.

### 3. Results and Discussion

#### 3.1 Inhibition studies on AChE and BuChE

The inhibitory activity of our synthetic derivatives was evaluated against AChE and BuChE using the method of Ellman et al. [38] with tacrine as a positive control. Their  $\text{IC}_{50}$  values and selectivity index for the inhibition of AChE and BuChE are summarized in Table 1. All these compounds were tested in five concentrations limited up to 100  $\mu\text{M}$ , resulting in ranged from 20% to 80% enzyme inhibition. For comparison, tacrine and previously reported compounds **9e-9g** were tested under the same experimental conditions. As shown in

Table 1, all synthetic derivatives showed high inhibitory activity and good inhibition selectivity against AChE over BuChE. Compounds **9a** and **9b** displayed the most potent inhibitory activity and inhibition selectivity for AChE, with their IC<sub>50</sub> values of 0.76 nM and 0.60 nM, and selectivity indexes of 3225 and 3092, respectively.

Comparing with the positive control and previously synthesized compounds **9e–9g**, the inhibitory activity of compounds **9a** and **9b** was 160–180-fold better than tacrine, and 100–120-fold better than **9e–9g**. Simultaneously, their inhibition selectivity for AChE increased about 10-fold compared with compounds **9e–9g** (Table 1). To investigate whether the improvement was due to the *N*-heteroaromatic ring or the positive charge, we designed and synthesized derivatives **10m** and **10n** with the aliphatic ring or alkyl quaternary ammonium at the end of side chain. The result showed a 2~3 times decrease in activity for **10m** and **10n** comparing with the corresponding compounds without positive charges, **10d** and **10f**. It indicated that the terminal *N*-heteroaromatic ring played an important role in enhancing their inhibitory potency and selectivity against AChE. And it also might be the reason why our novel compounds have higher activity and selectivity for AChE than those reported before [34]. In order to further confirm the role of *N*-heteroaromatic ring, we also synthesized several derivatives with phenyl or pyridyl group at the end of side chain, including compounds **9j–9l**, **10j–10l**, and **11l**, it was found that compounds (**9j** and **10j**) with pyridyl group had better activity than those with phenyl group. This result told us that the electron density of aromatic ring might be associated with the inhibitory activity.

On the other hand, we also investigated the effects of the side chain length on inhibitory ability of AChE. As shown in Table 1, two series of compounds (**9a–9i**, **9l** and **10a–10i**, **10l**), which had a linkage of one or two atoms ( $n = 1$  or  $n = 2$ ) in side chain respectively, did not show significant difference in their inhibitory activity.

But when the side chain length was further increased to three atoms, it showed a decrease on inhibitory activity. For example, compared with **9a** and **10a** ( $IC_{50}$  for AChE, 0.8 nM and 2.3 nM respectively), the activity of **11a** ( $IC_{50}$  for AChE, 3.9 nM) with a linker of three methylene groups had about 20-fold and 1.7-fold decrease, respectively. And the activities of other compounds **10j~10k**, **11c**, **11f**, and **11l** were also correspondingly lower than those of compounds **9j~9k**, **10c**, **10f**, and **10l**. Therefore, the linkage with 1 to 2 atoms seems to be in favor of inhibition for AChE.

### 3.2 Kinetic studies for the inhibition of AChE

Compounds **9b** and **10f** with different structures (with or without a positive charge) had the best inhibitory activity for AChE, which were further studied by graphical analysis of their steady-state inhibition data, as shown in Figure 2. The Lineweaver-Burk plots showed that both inhibitions had rising slopes and increasing intercepts at higher inhibitor concentration, which indicated a mixed-type inhibition. It was shown that compounds **9b** and **10f** could bind to both catalytic active site (CAS) and PAS of AChE, which are similar to that of tacrine and consistent with our results of molecular modeling study.

### 3.3 Molecular modeling study

To investigate the interacting mode between our synthetic compounds and *TcAChE* (PDB code: 1ACJ), a molecular modeling study utilizing the docking program named AUTODOCK 4.0 package with Discovery Studio 2.5 was carried out [39, 40]. The results of docking showed that our synthetic compounds displayed multiple binding patterns with *TcAChE*, as shown in Figure 3A. In the *TcAChE-9b* complex, the 7,8-dehydrorutaecarpine moiety occupied the PAS of enzyme and possessed potential hydrophobic interaction with residues Tyr334, Phe330, Phe290 and Tyr121. Moreover, it might induce  $\pi$ - $\pi$  interactions with these

residues when the bond of these residues rotated. The linker was long enough for the pyridyl substituted group arriving in the CAS of AChE, causing potential  $\pi$ -cation interaction and hydrophobic interaction with residues Trp84 and Tyr130. But the compounds with a too long linker (3 atoms) will result in the overcrowding of CAS domain and change the binding mode of whole molecule. The results of docking explained why the compounds with terminal N-heteroaromatic ring in the side chain and appropriate length of linker have higher inhibition potency against AChE, and were consistent with results of structure-activity relationship of our synthesized compounds for AChE mentioned above. The simultaneously binding of **9b** with the peripheral site and active gorge of *Tc*AChE explained the promising potency for AChE inhibition and revealed a mixed-type inhibition of compound. In addition, we also performed a docking between **9b** and *Hu*BuChE (PDB code: 1POI) using same program. As shown in Figure 3B, it was found that the 7,8-dehydrorutaecarpine moiety entered the catalytic active site of BuChE and interact with residue Asp200. No other notably interaction was observed between **9b** and *Hu*BuChE, giving the reason for weaker inhibition of compounds on BuChE and higher selectivity for AChE.

#### 3.4 Inhibition of self and AChE-induced $A\beta(1-42)$ aggregation

The inhibition of self and AChE-induced amyloid-beta (1-42) ( $A\beta_{1-42}$ ) aggregation by our synthetic derivatives was determined by using thioflavin T (ThT) assay [41], with tacrine, curcumin, propidium iodide and Congo-red as reference compounds. Table 2 and Figure 4 summarized the data for their effects on  $A\beta_{1-42}$  peptide aggregation at concentration of 25  $\mu$ M. In the ThT assay screening for  $A\beta_{1-42}$  peptide self-aggregation inhibition, the most potent compounds were found to be **10a-10b**, **11a** and **11c** with respective inhibition ratio of 61%, 54%, 60% and 55%, which are higher than that of curcumin (51%). The activities of other compounds are similar or lower than that of curcumin. To further explore the dual effects of these compounds,

AChE-induced  $A\beta_{1-42}$  aggregation inhibitory activity was examined based on the same ThT assay.  $A\beta$  deposition in AD brain has been linked to AChE expression, and the PAS of AChE can bind to the  $A\beta$ , accelerating the formation of amyloid fibrils [20]. Thus, inhibition of AChE, especially inhibition of PAS of AChE, might affect  $A\beta$  aggregation. As shown in Table 2 and Figure 4, tacrine, which had higher affinity for CAS than for PAS of AChE, showed a small effect (about 5% at 25  $\mu\text{M}$ ) against AChE-induced  $A\beta_{1-42}$  aggregation. However, propidium iodide significantly reduced  $A\beta_{1-42}$  aggregation (about 85%) as a result of its noncompetitive inhibition type. Remarkably, all of our synthetic derivatives showed good inhibitory potency against AChE-induced  $A\beta_{1-42}$  aggregation ranging from 75.9% to 92.8%, being 15.3- to 18.6-fold more effective than tacrine and 2.2- to 2.7-fold more effective than curcumin. Besides, compounds **9a-9c**, **9j**, **10a-10c**, **11a** and **11c** showed higher inhibitory activity against AChE-induced  $A\beta_{1-42}$  aggregation than propidium iodide and our previous compounds **9e-9g**, with inhibition ratio of 92.8%, 90.6%, 90.0%, 87.9%, 90.3%, 89.6%, 87.0%, 90.1% and 88.4%, respectively. Interestingly, this result is consistent with the outcome of inhibition against AChE and the previous study that the pyridinium-type compounds have shown high dual inhibitory potency against AChE and  $A\beta$  aggregation [42].

### 3.5 Studies of antioxidative activity

The reduction of the oxidative stress is another crucial aspect in designing agents for AD treatment. We examined the antioxidative activities of part of our synthetic derivatives and the oxygen radical absorbance capacity (ORAC) method was used. Their ability to scavenge radicals was shown as Trolox (a vitamin E analogue) equivalent, with their relative potency at concentration of 1 and 5  $\mu\text{M}$  compared to that of Trolox (shown in Table 2). The data showed that all the tested derivatives had better antioxidative activity ranging from 1.5- to 3.9-fold of Trolox, as a result for the introduction of the carbazole moiety to the backbone, giving

high antioxidative potency [36]. Furthermore, compounds **9d–9i** and **10d–10i** showed higher antioxidative activities than compounds **9a–9c**, **10a–10c** and **10m–10n**. It indicated that the positive charge of side chain may weaken the antioxidative activity of compounds, and aliphatic side chains are more important than aromatic side chains for enhancing their antioxidative activity.

### 3.6 Studies of metal-chelating properties

The chelation activity of the most potent compound **9b** for biometals such as  $\text{Na}^+$ ,  $\text{K}^+$ ,  $\text{Mg}^{2+}$ ,  $\text{Ca}^{2+}$ ,  $\text{Cu}^{2+}$ ,  $\text{Fe}^{2+}$ , and  $\text{Zn}^{2+}$  was studied by using UV-vis spectrometry. The UV absorption of compound **9b** in ethanol changed with the titration of  $\text{Cu}^{2+}$ ,  $\text{Fe}^{2+}$  and  $\text{Zn}^{2+}$ , while little change occurred after titrating with  $\text{Na}^+$ ,  $\text{K}^+$ ,  $\text{Mg}^{2+}$ ,  $\text{Ca}^{2+}$ . The maximum change in absorption intensity can be observed after adding  $\text{CuSO}_4$ , followed by  $\text{ZnSO}_4$  and  $\text{FeSO}_4$  (shown in Fig. 5A), indicating the formation of complex **9b**-metal (II). The molar ratio method was performed to determine the stoichiometry of the complex **9b**-metal (II) by titrating the ethanol solution of compound **9b** with ascending amounts of  $\text{CuSO}_4$  [43]. The UV spectra were recorded and treated by numerical subtraction of  $\text{CuSO}_4$  and **9b** at corresponding concentrations, plotted versus the mole fraction of **9b**. As shown in Figure 5B, the absorption firstly increased at 416 nm and then reached saturation point versus the mole proportion of  $\text{Cu}^{2+}$  to **9b**. The point for the two straight lines to intersect was determined to be at the mole proportion of 1.04, indicating 1:1 stoichiometry of the ligand-metal (II) complexes.

### 3.7 Studies of cytotoxic effects on SH-SY5Y

To determine the potential cytotoxic effects of our synthetic derivatives, the human neuroblastoma cell line SH-SY5Y was treated with part of our lead compounds at 0.1, 1.0, 10, and 100  $\mu\text{M}$  for 48h. The cell viability was calculated by using MTT colorimetry. As shown in Table 2, compounds **9a–9c** and **10a–10c** with higher

inhibitory activity on AChE and AChE-induced  $A\beta_{1-42}$  aggregation showed negligible cell death and higher  $IC_{50}$  values (above 100  $\mu M$ ) than that of curcumin (38  $\mu M$ ) under the same experimental conditions, indicating their lower neural cytotoxic effects.

#### 4. Conclusion

In summary, twenty seven new 3-aminoalkanamido-substituted 7,8-dehydrorutaecarpine derivatives **9a-9d**, **9h-9l**, **10a-10n**, **11a**, **11c**, **11f** and **11l** were synthesized and characterized as multifunctional anti-Alzheimer agents. All of these synthetic compounds showed high AChE inhibitory potency and good selectivity for AChE over BuChE. Structure-activity relationship analysis showed that the introduction of *N*-heteroaromatic ring at the end of their side chain was crucial to their inhibitory potency and selectivity against AChE. For example, the most potent compounds **9a-9c**, **9j**, **10a-10c**, **11a** and **11c** possessed better inhibitory activity ( $IC_{50}$  for AChE, 0.6-11.7 nM) and higher inhibition selectivity for AChE (Selectivity index ranged from 701 to 3225) than those of compounds with phenylic or aliphatic side chains. Moreover, the positive charge of side chains perhaps had little effect on their inhibitory activity and selectivity for AChE according to **9j** (3.9 nM) and **10a** (2.3 nM) having similar inhibitory activity for AChE. It showed a decrease on inhibitory activity with increasing side chain length to a linkage of 3 atoms and indicated that the linker with 1 or 2 atoms was in favor of inhibition for AChE. Both the inhibition kinetic analysis and molecular modeling study suggested that representative compounds **9b** and **10f** showed mixed-type inhibition, which figured out that compounds could bind to both CAS and PAS of AChE, inducing strong inhibitory effect and selectivity for AChE. In addition, all these lead compounds showed high effective activity of inhibiting AChE-induced  $A\beta_{1-42}$  aggregation than curcumin, especially compounds **9a-9c**, **9j**, **10a-10c**, **11a** and **11c** (ranged from 2.5- to 2.7-fold of curcumin). This result is consistent with the outcome for their inhibition against AChE. Furthermore, these lead

compounds could be metal chelators with better antioxidative property than Trolox due to the carbazole moiety of backbone and the introduction of side chain. The positive charge of side chain may weaken their antioxidative activity, and aliphatic side chains are more important than aromatic side chains for their antioxidative activity. Considering their low cytotoxicity, our results indicate that our new compounds provide good templates for development of new multi-functional anti-AD agents.

## 5. Experimental Section

### 5.1 Chemistry

$^1\text{H}$  and  $^{13}\text{C}$  NMR spectra were recorded using TMS as the internal standard in DMSO- $d_6$  or  $\text{CDCl}_3$  with a Bruker BioSpin GmbH spectrometer at 400 MHz and 100 MHz, respectively. High resolution mass spectra (HRMS) were recorded on Shimadzu LCMS-IT-TOF spectrometer. The purities of synthesized compounds were confirmed by using analytical HPLC with a dual pump Shimadzu LC-20AB system equipped with a Ultimate-QB-C18 column ( $4.6 \times 250$  mm,  $5 \mu\text{m}$ ) and eluted with methanol /water (60:40 to 70:30) containing 0.1% trifluoroacetic acid at a flow rate of 0.5 mL/min.

#### 5.1.2 General procedures for the preparation of compounds **7a**–**7c**

Intermediates **7a**–**7c** were prepared following the procedure previously reported [34].

##### 5.1.2.1 3-(2-Chloro-acetamino)-rutaecarpine (**7a**)

The compound **6** was reacted with chloroacetyl chloride following the general acylation procedure to give the desired product **7a** as a yellow solid in 83% yield.  $^1\text{H}$  NMR (400 MHz, DMSO):  $\delta$  11.81 (s, 1H), 10.73 (s, 1H), 8.49 (d,  $J = 2.3$  Hz, 1H), 7.99 (dd,  $J = 8.8, 2.5$  Hz, 1H), 7.66 (dd,  $J = 13.4, 8.4$  Hz, 2H), 7.48 (d,  $J = 8.2$  Hz,

1H), 7.26 (t,  $J = 7.6$  Hz, 1H), 7.09 (t,  $J = 7.5$  Hz, 1H), 4.46 (t,  $J = 6.8$  Hz, 2H), 4.30 (d,  $J = 18.0$  Hz, 2H), 3.18 (t,  $J = 6.8$  Hz, 2H); HRMS (ESI): calcd for (M+H)<sup>+</sup> (C<sub>20</sub>H<sub>15</sub>N<sub>4</sub>O<sub>2</sub>Cl) 379.0963, found 379.0941. These data are consistent with those reported previously [34].

#### 5.1.2.2 3-(2-Chloro-propionamino)-rutaecarpine (**7b**)

The compound **6** was reacted with 3-chloropropionyl chloride following the general acylation procedure to give the desired product **7b** as a yellow solid in 81% yield. <sup>1</sup>H NMR (400 MHz, DMSO):  $\delta$  11.81 (s, 1H), 10.49 (s, 1H), 8.51 (d,  $J = 2.0$  Hz, 1H), 8.01 (dd,  $J = 8.8, 2.3$  Hz, 1H), 7.65 (t,  $J = 8.3$  Hz, 2H), 7.48 (d,  $J = 8.2$  Hz, 1H), 7.26 (t,  $J = 7.6$  Hz, 1H), 7.09 (t,  $J = 7.5$  Hz, 1H), 4.46 (t,  $J = 6.8$  Hz, 2H), 3.92 (t,  $J = 6.2$  Hz, 2H), 3.17 (dd,  $J = 16.2, 9.4$  Hz, 2H), 2.89 (t,  $J = 6.2$  Hz, 2H); HRMS (ESI): calcd for (M+H)<sup>+</sup> (C<sub>21</sub>H<sub>17</sub>N<sub>4</sub>O<sub>2</sub>Cl) 393.1118, found 393.1097. These data are consistent with those reported previously [34].

#### 5.1.2.3 3-(2-Chloro-butylamino)-rutaecarpine (**7c**)

The compound **6** was reacted with 4-Chlorobutyl chloride following the general acylation procedure to give the desired product **7c** as a yellow solid in 51% yield. <sup>1</sup>H NMR (400 MHz, DMSO):  $\delta$  11.86 (s, 1H), 10.35 (s, 1H), 8.51 (s, 1H), 7.98 (d,  $J = 8.7$  Hz, 1H), 7.66 (d,  $J = 8.8$  Hz, 2H), 7.48 (d,  $J = 8.0$  Hz, 1H), 7.34 – 7.24 (m, 1H), 7.10 (t,  $J = 6.6$  Hz, 1H), 4.45 (t,  $J = 6.4$  Hz, 2H), 3.73 (t,  $J = 6.4$  Hz, 2H), 3.26 – 3.11 (m, 2H), 2.54 (d,  $J = 8.2$  Hz, 2H), 2.08 (dt,  $J = 12.4, 6.4$  Hz, 2H); HRMS (ESI): calcd for (M+H)<sup>+</sup> (C<sub>22</sub>H<sub>19</sub>N<sub>4</sub>O<sub>2</sub>Cl) 407.1218, found 407.1107.

#### 5.1.3 General procedures for the preparation of compounds **12a–12c**

A suspension of EDCI (1-(3-dimethylaminopropyl)-3-ethylcarbodiimide hydrochloride, 1.32 mmol) with the

appropriate aromatic acid (0.66 mmol) in tetrahydrofuran (20 mL) was stirred for 30 min at room temperature, then added the DIPEA (N,N-diisopropylethylamine, 1.32 mmol) to form a clear solution. The compound **6** (0.33 mmol) was dissolved in THF (10 mL) and dropped into the forementioned solution. The solvent was evaporated after stirring for 48h, filtered after adding ice water (50 mL), and then evaporated under vacuum. The resulting crude product was purified by using flash chromatography with petroleum ether/ acetic ether as elution solvent to afford **12a~12c**.

#### 5.1.3.1 3-(2-Phenyl-acetamino)-rutaecarpine (**12a**)

The compound **6** was reacted with phenylacetic acid following the general condensation procedure to give the desired product **12a** as a yellow solid in 78% yield. <sup>1</sup>H NMR (400 MHz, DMSO):  $\delta$  11.84 (s, 1H), 10.28 (s, 1H), 8.37 (s, 1H), 7.88 (d,  $J = 9.5$  Hz, 1H), 7.63 (d,  $J = 8.5$  Hz, 2H), 7.42 (t,  $J = 6.9$  Hz, 2H), 7.29 (d,  $J = 6.0$  Hz, 4H), 7.20 (d,  $J = 6.1$  Hz, 1H), 7.14 – 7.05 (m, 1H), 4.49 – 4.40 (m, 2H), 3.19 – 3.11 (m, 2H), 3.00 – 2.90 (m, 2H); HRMS (ESI): calcd for (M+H)<sup>+</sup> (C<sub>26</sub>H<sub>20</sub>N<sub>4</sub>O<sub>2</sub>) 421.1608, found 421.1567.

#### 5.1.3.2 3-(2-Phenyl-propionamino)-rutaecarpine (**12b**)

The compound **6** was reacted with 3-phenylpropionic acid following the general condensation procedure to give the desired product **12b** as a yellow solid in 69% yield. <sup>1</sup>H NMR (400 MHz, DMSO):  $\delta$  11.84 (s, 1H), 10.28 (s, 1H), 8.47 (s, 1H), 7.98 (d,  $J = 9.5$  Hz, 1H), 7.65 (d,  $J = 8.5$  Hz, 2H), 7.47 (t,  $J = 6.9$  Hz, 2H), 7.29 (d,  $J = 6.0$  Hz, 4H), 7.20 (d,  $J = 6.1$  Hz, 1H), 7.14 – 7.05 (m, 1H), 4.49 – 4.40 (m, 2H), 3.21 – 3.11 (m, 2H), 3.00 – 2.90 (m, 2H), 2.72 – 2.64 (m, 2H); HRMS (ESI): calcd for (M+H)<sup>+</sup> (C<sub>27</sub>H<sub>22</sub>N<sub>4</sub>O<sub>2</sub>) 435.1823, found 435.1767.

#### 5.1.3.3 3-(2-Phenyl-butiramino)-rutaecarpine (**12c**)

The compound **6** was reacted with 4-phenylbutyric acid following the general condensation procedure to give the desired product **12c** as a yellow solid in 81% yield. <sup>1</sup>H NMR (400 MHz, DMSO):  $\delta$  11.70 (s, 1H), 10.24 (s, 1H), 8.50 (s, 1H), 7.99 (d,  $J = 10.0$  Hz, 1H), 7.63 (dd,  $J = 14.3, 8.2$  Hz, 2H), 7.53 – 7.42 (m, 2H), 7.33 – 7.23 (m, 3H), 7.19 (d,  $J = 7.6$  Hz, 1H), 7.13 – 7.03 (m, 2H), 5.67 (s, 2H), 4.51 – 4.37 (m, 2H), 3.22 – 3.10 (m, 2H), 2.11 (d,  $J = 9.0$  Hz, 2H), 1.97 – 1.89 (m, 2H); HRMS (ESI): calcd for (M+H)<sup>+</sup> (C<sub>28</sub>H<sub>24</sub>N<sub>4</sub>O<sub>2</sub>) 449.1953, found 449.1687.

#### 5.1.4 General procedures for the preparation of compounds **8a–8c**, **9l**, **10l** and **11l**

A solution of DDQ (2,3-dichloro-5,6-dicyano-1,4-benzoquinone, 5.2 mmol) in dioxane (10 mL) was dropped to a hot solution of intermediates **7a–7c** or **12a–12c** (2.5 mmol) in DMSO (1.0 mL) and dioxane (250 mL) for 30 min. The solvent was evaporated after a reflux for 12h, and the residue was washed by a solution of KOH (1.5g) in water (25 mL) until all DDQ-2H was cleared. The resulting crude product was purified by recrystallization from EtOH/DMF (5:1 v/v). The product was characterized, and the data of **8a–8b** are consistent with those reported previously [34].

##### 5.1.4.1 3-(2-Chloro-acetamino)-7,8-dehydrorutaecarpine (**8a**)

The compound **7a** was reacted with DDQ following the general dehydrogenation procedure to give the desired product **8a** as a green solid in 86% yield. <sup>1</sup>H NMR (400 MHz, DMSO):  $\delta$  12.68 (s, 1H), 10.69 (s, 1H), 8.72 (d,  $J = 0.8$  Hz, 1H), 8.63 (d,  $J = 7.5$  Hz, 1H), 8.18 (d,  $J = 7.9$  Hz, 1H), 8.08 (d,  $J = 7.8$  Hz, 1H), 7.85 (dd,  $J = 10.6, 8.7$  Hz, 2H), 7.69 (d,  $J = 8.1$  Hz, 1H), 7.50 (t,  $J = 7.3$  Hz, 1H), 7.30 (t,  $J = 7.3$  Hz, 1H), 4.34 (s, 2H); HRMS (ESI): calcd for (M+H)<sup>+</sup> (C<sub>20</sub>H<sub>13</sub>N<sub>4</sub>O<sub>2</sub>Cl) 377.0805, found 377.0763. These data are consistent with those reported previously [34].

#### 5.1.4.2 3-(2-Chloro-propionamino)-7,8-dehydrorutaecarpine (**8b**)

The compound **7b** was reacted with DDQ following the general dehydrogenation procedure to give the desired product **8b** as a green solid in 85% yield. <sup>1</sup>H NMR (400 MHz, DMSO): δ 12.78 (s, 1H), 10.53 (s, 1H), 8.77 (d, *J* = 1.8 Hz, 1H), 8.66 (d, *J* = 7.5 Hz, 1H), 8.21 (d, *J* = 7.9 Hz, 1H), 8.11 (dd, *J* = 8.9, 2.1 Hz, 1H), 7.89 (t, *J* = 7.2 Hz, 2H), 7.71 (d, *J* = 8.2 Hz, 1H), 7.53 (t, *J* = 7.5 Hz, 1H), 7.32 (t, *J* = 7.6 Hz, 1H), 3.94 (t, *J* = 6.2 Hz, 2H), 2.92 (t, *J* = 6.1 Hz, 2H); HRMS (ESI): calcd for (M+H)<sup>+</sup> (C<sub>21</sub>H<sub>15</sub>N<sub>4</sub>O<sub>2</sub>Cl) 391.0905, found 391.0863.

#### 5.1.4.3 3-(2-Chloro-butylamino)-7,8-dehydrorutaecarpine (**8c**)

The compound **7c** was reacted with DDQ following the general dehydrogenation procedure to give the desired product **8c** as a green solid in 76% yield. <sup>1</sup>H NMR (400 MHz, DMSO): δ 12.86 (s, 1H), 10.46 (s, 0H), 8.76 (s, 0H), 8.68 (d, *J* = 7.0 Hz, 1H), 8.22 (d, *J* = 7.4 Hz, 1H), 8.10 (d, *J* = 8.9 Hz, 1H), 7.94 (d, *J* = 7.2 Hz, 1H), 7.88 (d, *J* = 8.8 Hz, 0H), 7.72 (d, *J* = 7.1 Hz, 1H), 7.58 – 7.51 (m, 1H), 7.33 (t, *J* = 7.6 Hz, 1H), 3.75 (t, *J* = 5.9 Hz, 1H), 2.64 – 2.54 (m, 1H), 2.17 – 2.03 (m, 1H); HRMS (ESI): calcd for (M+H)<sup>+</sup> (C<sub>22</sub>H<sub>17</sub>N<sub>4</sub>O<sub>2</sub>Cl) 405.1105, found 405.1033.

#### 5.1.4.4 3-(2-Phenyl-acetamino)-7,8-dehydrorutaecarpine (**9l**)

The compound **12a** was reacted with DDQ following the general dehydrogenation procedure to give the desired product **9l** as a brown solid in 86% yield. <sup>1</sup>H NMR (400 MHz, DMSO): δ 12.69 (s, 1H), 11.45 (s, 1H), 9.13 (d, *J* = 5.1 Hz, 2H), 8.76 (d, *J* = 7.5 Hz, 1H), 8.75 – 8.69 (m, 1H), 8.62 (d, *J* = 7.5 Hz, 2H), 8.26 (t, *J* = 6.8 Hz, 2H), 8.18 (d, *J* = 8.1 Hz, 2H), 8.10 (d, *J* = 9.6 Hz, 1H), 7.90 (s, 1H), 7.84 (d, *J* = 7.6 Hz, 1H), 7.70 (d, *J* = 8.2 Hz, 1H), 7.54 – 7.46 (m, 2H), 7.30 (t, *J* = 7.2 Hz, 2H), 5.79 (s, 2H); <sup>13</sup>C NMR (101 MHz, DMSO): δ

168.04, 158.28, 148.56, 143.68, 139.77, 139.03, 135.56, 129.42, 128.88, 127.14, 126.83, 126.35, 121.80, 120.65, 120.34, 119.24, 117.52, 116.02, 115.71, 114.90, 112.64, 112.08, 107.92, 40.71. Purity: 98.6% by HPLC. HRMS (ESI): calcd for (M+H)<sup>+</sup> (C<sub>26</sub>H<sub>18</sub>N<sub>4</sub>O<sub>2</sub>) 419.1545, found 419.1533.

#### 5.1.4.5 3-(2-Phenyl-propionamino)-7,8-dehydrorutaecarpine (**10l**)

The compound **12b** was reacted with DDQ following the general dehydrogenation procedure to give the desired product **10l** as a brown solid in 80% yield. <sup>1</sup>H NMR (400 MHz, DMSO): δ 11.83 (s, 1H), 10.55 (s, 1H), 8.48 (d, *J* = 2.1 Hz, 1H), 8.01 (dd, *J* = 8.8, 2.2 Hz, 1H), 7.65 (dd, *J* = 8.3, 5.2 Hz, 2H), 7.48 (s, 2H), 7.37 (t, *J* = 8.0 Hz, 3H), 7.31 – 7.23 (m, 3H), 7.17 – 7.02 (m, 2H), 4.45 (t, *J* = 6.7 Hz, 2H), 3.22 – 3.07 (m, 2H); <sup>13</sup>C NMR (101 MHz, DMSO): δ 169.50, 164.76, 158.28, 148.10, 139.82, 135.56, 135.10, 129.28, 128.89, 127.48, 126.62, 126.51, 121.79, 120.80, 120.46, 117.62, 116.58, 116.00, 115.35, 115.15, 112.68, 112.45, 108.07, 47.39, 43.53. Purity: 97.8% by HPLC. HRMS (ESI): calcd for (M+H)<sup>+</sup> (C<sub>27</sub>H<sub>20</sub>N<sub>4</sub>O<sub>2</sub>) 433.1615, found 433.1603.

#### 5.1.4.6 3-(2-Phenyl-butyramino)-7,8-dehydrorutaecarpine (**11l**)

The compound **12c** was reacted with DDQ following the general dehydrogenation procedure to give the desired product **11l** as a brown solid in 72% yield. <sup>1</sup>H NMR (400 MHz, DMSO): δ 11.83 (s, 1H), 10.24 (s, 1H), 8.50 (d, *J* = 2.3 Hz, 1H), 7.98 (dd, *J* = 8.7, 2.3 Hz, 1H), 7.73 – 7.60 (m, 2H), 7.55 – 7.42 (m, 2H), 7.30 (dd, *J* = 14.1, 6.7 Hz, 4H), 7.20 (dd, *J* = 10.1, 7.3 Hz, 2H), 7.15 – 7.00 (m, 2H), 4.51 – 4.41 (m, 2H), 3.24 – 3.12 (m, 2H), 2.45 – 2.34 (m, 2H); <sup>13</sup>C NMR (101 MHz, DMSO): δ 169.29, 160.31, 150.75, 143.96, 142.89, 138.54, 137.16, 135.75, 129.10, 128.28, 126.97, 126.84, 126.54, 126.02, 124.85, 124.55, 120.80, 119.76, 119.63, 117.39, 115.13, 112.43, 101.57, 43.28, 40.83, 18.87. Purity: 97.7% by HPLC. HRMS (ESI): calcd for

(M+H)<sup>+</sup> (C<sub>28</sub>H<sub>22</sub>N<sub>4</sub>O<sub>2</sub>) 447.1935, found 447.1813.

### 5.1.5 General procedures for the preparation of compounds **9a–9c**, **9j**, **10a–10c**, **10j**, **11a** and **11c**

A suspension of compounds **8a–8c** (1.0 mmol) in appropriate *N*-heterocyclic amine (12 mL) was heated under reflux for 8h, cooled to 0 °C, filtered after adding ether (30 mL), washed with ether, and then evaporated under vacuum. The resulting crude product was purified by recrystallization from EtOH/DMF (5:1 v/v) to afford **9a–9c**, **9j**, **10a–10c**, **10j**, **11a** and **11c**.

#### 5.1.5.1 3-(2-*N*-Pyridyl-acetamino)-7,8-dehydrorutaecarpine (**9a**)

The compound **8a** was reacted with pyridine following the general procedure to give the desired product **9a** as a brown solid in 64% yield. <sup>1</sup>H NMR (400 MHz, DMSO): δ 12.69 (s, 1H), 11.45 (s, 1H), 9.13 (d, *J* = 5.1 Hz, 2H), 8.76 (d, *J* = 7.5 Hz, 1H), 8.72 (d, *J* = 8.3 Hz, 1H), 8.60 (d, *J* = 15.9, 4.6 Hz, 1H), 8.26 (t, *J* = 6.8 Hz, 2H), 8.18 (d, *J* = 8.1 Hz, 1H), 8.10 (d, *J* = 9.6 Hz, 1H), 7.89 (d, *J* = 8.8 Hz, 1H), 7.84 (d, *J* = 7.6 Hz, 1H), 7.70 (d, *J* = 8.2 Hz, 1H), 7.54 – 7.46 (m, 1H), 7.30 (t, *J* = 7.2 Hz, 1H), 5.79 (s, 2H); <sup>13</sup>C NMR (101 MHz, DMSO): δ 163.45, 158.34, 146.47, 146.27, 144.14, 139.87, 139.35, 134.90, 129.45, 127.54, 127.25, 127.18, 126.57, 121.84, 120.83, 120.51, 119.52, 117.63, 116.11, 115.34, 112.71, 108.18, 62.76. Purity: 96.7% by HPLC. HRMS (ESI): calcd for (M)<sup>+</sup> (C<sub>25</sub>H<sub>18</sub>N<sub>5</sub>O<sub>2</sub>) 420.1455, found 420.1470.

#### 5.1.5.2 3-(2-(3-Fluoropyrid-1-yl)-acetamino)-7,8-dehydrorutaecarpine (**9b**)

The compound **8a** was reacted with 3-fluoropyridine following the general procedure to give the desired product **9b** as a brown solid in 89% yield. <sup>1</sup>H NMR (400 MHz, DMSO): δ 12.70 (s, 1H), 11.66 (s, 1H), 9.59 (s, 1H), 9.12 (d, *J* = 5.6 Hz, 1H), 8.80 (d, *J* = 13.2 Hz, 2H), 8.61 (d, *J* = 8.1 Hz, 1H), 8.39 (d, *J* = 7.4 Hz, 1H),

8.18 (d,  $J = 7.3$  Hz, 1H), 8.12 (d,  $J = 10.1$  Hz, 1H), 7.89 (d,  $J = 9.7$  Hz, 1H), 7.84 (d,  $J = 8.3$  Hz, 1H), 7.70 (d,  $J = 9.1$  Hz, 1H), 7.53 – 7.47 (m, 1H), 7.35 – 7.23 (m, 1H), 5.85 (s, 2H);  $^{13}\text{C}$  NMR (101 MHz, DMSO):  $\delta$  165.32, 163.31, 160.65, 158.84, 144.45, 140.47, 139.92, 137.21, 136.95, 135.25, 134.51, 129.94, 129.41, 127.86, 127.66, 127.09, 122.39, 121.28, 121.03, 118.15, 116.61, 116.14, 113.26, 108.67, 63.09. Purity: 97.8% by HPLC. HRMS (ESI): calcd for  $(\text{M})^+$  ( $\text{C}_{25}\text{H}_{17}\text{N}_5\text{O}_2\text{F}$ ) 438.1361, found 438.1347.

#### 5.1.5.3 3-(2-(1-Methylimidazol-3-yl)-acetamino)-7,8-dehydrorutaecarpine (**9c**)

The compound **8a** was reacted with 1-methylimidazole following the general procedure to give the desired product **9c** as a brown solid in 78% yield.  $^1\text{H}$  NMR (400 MHz, DMSO):  $\delta$  12.69 (s, 1H), 11.33 (s, 1H), 9.21 (s, 1H), 8.78 (s, 1H), 8.62 (d,  $J = 7.2$  Hz, 1H), 8.18 (d,  $J = 7.5$  Hz, 1H), 8.10 (d,  $J = 8.6$  Hz, 1H), 7.86 (dd,  $J = 16.2, 8.4$  Hz, 3H), 7.77 (s, 1H), 7.70 (d,  $J = 8.2$  Hz, 1H), 7.50 (t,  $J = 7.0$  Hz, 1H), 7.30 (t,  $J = 6.9$  Hz, 1H), 5.35 (s, 2H), 3.95 (s, 3H);  $^{13}\text{C}$  NMR (101 MHz, DMSO):  $\delta$  163.92, 158.22, 143.90, 139.78, 139.08, 137.93, 135.07, 129.34, 127.14, 126.88, 126.37, 123.88, 123.05, 121.76, 120.65, 120.33, 119.32, 117.46, 115.94, 115.14, 112.65, 107.91, 51.35, 35.86. Purity: 99.0% by HPLC. HRMS (ESI): calcd for  $(\text{M})^+$  ( $\text{C}_{24}\text{H}_{19}\text{N}_6\text{O}_2$ ) 423.1564, found 423.1568.

#### 5.1.5.4 3-(2-(Pyridin-3-yloxy)-acetamino)-7,8-dehydrorutaecarpine (**9j**)

The compound **8a** was reacted with 3-hydroxypyridine in DMSO (3 mL) following the general procedure to give the desired product **9j** as a brown solid in 98% yield.  $^1\text{H}$  NMR (400 MHz, DMSO):  $\delta$  12.70 (s, 1H), 11.50 (s, 1H), 8.76 (s, 1H), 8.61 (s, 2H), 8.55 (d,  $J = 27.5$  Hz, 1H), 8.13 (dd,  $J = 17.0, 7.3$  Hz, 2H), 8.07 – 8.02 (m, 1H), 7.98 (d,  $J = 4.0$  Hz, 1H), 7.83 (dd,  $J = 25.1, 6.9$  Hz, 2H), 7.69 (d,  $J = 7.7$  Hz, 1H), 7.50 (d,  $J = 0.8$  Hz, 1H), 7.30 (d,  $J = 6.9$  Hz, 1H), 5.69 (s, 2H);  $^{13}\text{C}$  NMR (101 MHz, DMSO):  $\delta$  163.38, 158.20, 144.19, 143.99,

139.79, 139.18, 134.81, 134.63, 132.01, 129.34, 127.76, 127.11, 127.02, 126.41, 121.77, 120.65, 120.38, 119.37, 117.52, 115.98, 115.22, 112.69, 108.02, 107.80, 62.03. Purity: 97.8% by HPLC. HRMS (ESI): calcd for (M-H)<sup>-</sup> (C<sub>25</sub>H<sub>17</sub>N<sub>5</sub>O<sub>3</sub>) 434.1259, found 434.1265.

#### 5.1.5.5 3-(2-N-Pyridyl-propionamino)-7,8-dehydrorutaecarpine (**10a**)

The compound **8b** was reacted with pyridine following the general procedure to give the desired product **10a** as a brown solid in 64% yield. <sup>1</sup>H NMR (400 MHz, DMSO): δ 12.70 (s, 1H), 10.93 (s, 1H), 9.23 (d, *J* = 4.5 Hz, 2H), 8.74 (s, 1H), 8.60 (d, *J* = 7.4 Hz, 2H), 8.19 (d, *J* = 6.1 Hz, 3H), 8.04 (d, *J* = 8.4 Hz, 1H), 7.83 (s, 2H), 7.68 (d, *J* = 7.8 Hz, 1H), 7.49 (t, *J* = 6.5 Hz, 1H), 7.29 (t, *J* = 6.7 Hz, 1H), 4.98 (s, 2H), 3.29 (s, 2H); <sup>13</sup>C NMR (101 MHz, DMSO): δ 168.49, 158.82, 146.22, 145.89, 140.36, 139.59, 135.97, 129.80, 128.28, 127.88, 127.19, 127.10, 122.31, 121.34, 121.02, 120.04, 118.14, 116.48, 115.51, 113.21, 108.67, 57.37, 37.10. Purity: 99.2% by HPLC. HRMS (ESI): calcd for (M)<sup>+</sup> (C<sub>26</sub>H<sub>20</sub>N<sub>5</sub>O<sub>2</sub>) 434.1612, found 434.1608.

#### 5.1.5.6 3-(2-(3-Fluoropyrid-1-yl))-propionamino)-7,8-dehydrorutaecarpine (**10b**)

The compound **8b** was reacted with 3-fluoropyridine following the general procedure to give the desired product **10b** as a brown solid in 60% yield. <sup>1</sup>H NMR (400 MHz, DMSO): δ 12.70 (s, 1H), 10.93 (s, 1H), 9.23 (d, *J* = 4.5 Hz, 2H), 8.74 (s, 1H), 8.61 (s, 1H), 8.19 (d, *J* = 6.1 Hz, 3H), 8.04 (d, *J* = 8.4 Hz, 1H), 7.83 (s, 2H), 7.68 (d, *J* = 7.8 Hz, 1H), 7.49 (t, *J* = 7.0 Hz, 1H), 7.29 (t, *J* = 6.7 Hz, 1H), 4.98 (m, 2H), 3.29 (m, 2H); <sup>13</sup>C NMR (101 MHz, DMSO): δ 165.32, 163.31, 160.65, 158.84, 144.45, 140.47, 139.92, 137.21, 136.95, 135.25, 134.51, 129.94, 129.41, 127.86, 127.66, 127.09, 122.39, 121.28, 121.03, 118.15, 116.61, 116.14, 113.26, 108.67, 63.09, 44.00. Purity: 98.8% by HPLC. HRMS (ESI): calcd for (M)<sup>+</sup> (C<sub>26</sub>H<sub>19</sub>N<sub>5</sub>O<sub>2</sub>F) 452.1517, found 452.1530.

#### 5.1.5.7 3-(2-(1-Methylimidazol-3-yl)-propionamino)-7,8-dehydrorutaecarpine (**10c**)

The compound **8b** was reacted with 1-methylimidazole following the general procedure to give the desired product **10c** as a brown solid in 56% yield. <sup>1</sup>H NMR (400 MHz, DMSO):  $\delta$  12.69 (s, 1H), 10.93 (s, 1H), 9.27 (s, 1H), 8.80 (s, 1H), 8.61 (d,  $J = 7.5$  Hz, 1H), 8.17 (d,  $J = 7.9$  Hz, 1H), 8.08 (d,  $J = 8.0$  Hz, 1H), 7.87 – 7.80 (m, 3H), 7.74 – 7.66 (m, 2H), 7.49 (t,  $J = 7.6$  Hz, 1H), 7.30 (t,  $J = 7.4$  Hz, 1H), 4.54 (s, 2H), 3.88 (s, 3H), 3.12 (s, 2H); <sup>13</sup>C NMR (101 MHz, DMSO):  $\delta$  168.19, 158.32, 143.73, 139.81, 139.06, 137.06, 135.63, 129.45, 127.36, 126.75, 126.42, 123.46, 122.48, 121.82, 120.72, 120.41, 119.27, 117.55, 115.98, 114.93, 112.68, 108.00, 44.97, 35.97, 35.72. Purity: 99.3% by HPLC. HRMS (ESI): calcd for (M)<sup>+</sup> (C<sub>25</sub>H<sub>21</sub>N<sub>6</sub>O<sub>2</sub>) 437.1721, found 437.1729.

#### 5.1.5.8 3-(2-(Pyridin-3-yloxy)-acetamino)-7,8-dehydrorutaecarpine (**10j**)

The compound **8b** was reacted with 3-hydroxypyridine in DMSO (3 mL) following the general procedure to give the desired product **10j** as a brown solid in 91% yield. <sup>1</sup>H NMR (400 MHz, DMSO):  $\delta$  12.71 (s, 1H), 10.77 (s, 1H), 8.75 (s, 1H), 8.67 (s, 1H), 8.61 (d,  $J = 7.8$  Hz, 1H), 8.17 (d,  $J = 7.8$  Hz, 1H), 8.02 (d,  $J = 7.9$  Hz, 2H), 7.97 (d,  $J = 6.4$  Hz, 1H), 7.83 (d,  $J = 7.2$  Hz, 2H), 7.68 (d,  $J = 7.9$  Hz, 1H), 7.52 – 7.47 (m, 1H), 7.35 – 7.25 (m, 1H), 4.90 (d,  $J = 0.6$  Hz, 2H), 3.24 (d,  $J = 1.0$  Hz, 2H); <sup>13</sup>C NMR (101 MHz, DMSO):  $\delta$  167.76, 158.17, 156.90, 143.56, 139.71, 138.90, 135.95, 135.35, 133.30, 131.47, 129.26, 128.18, 127.14, 126.64, 126.35, 121.69, 120.61, 120.32, 119.27, 117.46, 115.84, 114.82, 112.60, 107.90, 56.82, 36.81. Purity: 99.6% by HPLC. HRMS (ESI): calcd for (M+H)<sup>+</sup> (C<sub>26</sub>H<sub>19</sub>N<sub>5</sub>O<sub>3</sub>) 450.1561, found 450.1548.

#### 5.1.5.9 3-(2-N-Pyridyl-butylamino)-7,8-dehydrorutaecarpine (**11a**)

The compound **8c** was reacted with pyridine following the general procedure to give the desired product **11a** as a brown solid in 79% yield. <sup>1</sup>H NMR (400 MHz, DMSO):  $\delta$  12.70 (s, 1H), 10.48 (s, 1H), 9.16 (d,  $J$  = 5.7 Hz, 2H), 8.73 (s, 1H), 8.62 (d,  $J$  = 6.6 Hz, 2H), 8.26 – 8.13 (m, 3H), 8.04 (d,  $J$  = 8.8 Hz, 1H), 7.84 (d,  $J$  = 8.1 Hz, 2H), 7.69 (d,  $J$  = 8.3 Hz, 1H), 7.57 – 7.46 (m, 1H), 7.36 – 7.25 (m, 1H), 4.73 (t,  $J$  = 7.6 Hz, 2H), 2.49 – 2.41 (m, 2H), 2.37 – 2.29 (m, 2H); <sup>13</sup>C NMR (101 MHz, DMSO):  $\delta$  169.29, 160.31, 150.75, 143.96, 142.89, 138.54, 137.16, 135.75, 129.10, 128.28, 126.97, 126.54, 126.02, 124.85, 124.55, 120.80, 119.76, 119.63, 117.39, 115.13, 112.43, 101.57, 43.28, 40.83, 18.87. Purity: 98.9% by HPLC. HRMS (ESI): calcd for (M)<sup>+</sup> (C<sub>27</sub>H<sub>22</sub>N<sub>5</sub>O<sub>2</sub>) 448.1768, found 448.1774.

#### 5.1.5.10 3-(2-(1-Methylimidazol-3-yl)-butyramino)-7,8-dehydrorutaecarpine (**11c**)

The compound **8c** was reacted with 1-methylimidazole following the general procedure to give the desired product **11c** as a brown solid in 50% yield. <sup>1</sup>H NMR (400 MHz, DMSO):  $\delta$  12.69 (s, 1H), 10.45 (s, 1H), 9.20 (s, 1H), 8.76 (s, 1H), 8.61 (d,  $J$  = 6.2 Hz, 1H), 8.17 (d,  $J$  = 6.4 Hz, 1H), 8.09 – 8.00 (m, 1H), 7.83 (s, 2H), 7.77 – 7.64 (m, 3H), 7.57 – 7.41 (m, 1H), 7.37 – 7.23 (m, 1H), 4.28 (t,  $J$  = 11.4 Hz, 2H), 3.85 (s, 3H), 2.23 – 2.10 (m, 2H), 1.91 (t,  $J$  = 5.3 Hz, 2H); <sup>13</sup>C NMR (101 MHz, DMSO):  $\delta$  171.90, 158.28, 143.55, 139.76, 138.95, 129.38, 127.78, 127.27, 126.56, 126.38, 123.59, 122.32, 121.77, 120.81, 120.62, 120.39, 117.52, 116.68, 112.62, 112.49, 107.94, 99.49, 48.54, 35.73, 31.23, 20.98. Purity: 98.7% by HPLC. HRMS (ESI): calcd for (M)<sup>+</sup> (C<sub>26</sub>H<sub>23</sub>N<sub>6</sub>O<sub>2</sub>) 451.1877, found 451.1854.

#### 5.1.6 General procedures for the preparation of compounds **9d–9i**, **9k**, **10d–10i**, **10k** and **11f**

The appropriate secondary amine (1.0 mL) was added to a suspension of compounds **8a–8c** (1.0 mmol) and NaI (0.15 g) in EtOH (30 mL). After a reflux for 8h, the mixture was cooled to 0 °C, filtered, washed with

EtOH and water, and then evaporated under vacuum. The resulting crude product was purified by using flash chromatography with chloroform/methanol as elution solvent. Compounds **9e**–**9g** were synthesized, and their characterization data are consistent with those reported previously [34].

#### 5.1.6.1 3-(2-Dimethylamino-acetamino)-7,8-dehydrorutaecarpine (**9d**)

The compound **8a** was reacted with excess dimethylamine following the general procedure to give the desired product **9d** as a yellow solid in 71% yield. <sup>1</sup>H NMR (400 MHz, DMSO):  $\delta$  12.67 (s, 1H), 10.15 (s, 1H), 8.80 (d,  $J = 2.0$  Hz, 1H), 8.62 (d,  $J = 7.5$  Hz, 1H), 8.17 (d,  $J = 8.1$  Hz, 2H), 7.85 – 7.79 (m, 2H), 7.69 (d,  $J = 8.1$  Hz, 1H), 7.49 (t,  $J = 7.6$  Hz, 1H), 7.30 (t,  $J = 7.5$  Hz, 1H), 3.16 (s, 2H), 2.33 (s, 6H); <sup>13</sup>C NMR (101 MHz, DMSO):  $\delta$  168.88, 158.36, 143.77, 139.82, 139.11, 135.46, 129.47, 127.80, 126.55, 121.86, 120.73, 120.42, 119.29, 117.60, 116.02, 115.43, 112.68, 107.98, 63.26, 45.33. Purity: 99.8% by HPLC. HRMS (ESI): calcd for (M+H)<sup>+</sup> (C<sub>22</sub>H<sub>19</sub>N<sub>5</sub>O<sub>2</sub>) 386.1612, found 386.1621.

#### 5.1.6.2 3-(2-N-Morpholinyl-acetamino)-7,8-dehydrorutaecarpine (**9h**)

The compound **8a** was reacted with excess morpholine following the general procedure to give the desired product **9h** as a yellow solid in 80% yield. <sup>1</sup>H NMR (400 MHz, DMSO):  $\delta$  12.67 (s, 1H), 10.15 (s, 1H), 8.73 (d,  $J = 12.1$  Hz, 1H), 8.62 (d,  $J = 7.2$  Hz, 1H), 8.20 – 8.13 (m, 2H), 7.87 – 7.80 (m, 2H), 7.69 (d,  $J = 8.1$  Hz, 1H), 7.49 (t,  $J = 7.5$  Hz, 1H), 7.30 (t,  $J = 7.1$  Hz, 1H), 3.67 (s, 4H), 3.21 (s, 2H), 2.56 (s, 4H); <sup>13</sup>C NMR (101 MHz, DMSO):  $\delta$  168.30, 158.36, 143.83, 139.83, 139.14, 135.30, 129.47, 127.80, 126.71, 126.44, 121.86, 120.74, 120.43, 119.32, 117.61, 116.02, 115.49, 112.69, 108.00, 66.05, 62.05, 53.17. Purity: 99.5% by HPLC. HRMS (ESI): calcd for (M+H)<sup>+</sup> (C<sub>24</sub>H<sub>21</sub>N<sub>5</sub>O<sub>3</sub>) 428.1717, found 428.1736.

### 5.1.6.3 3-(2-(4-Methylpiperazin-1-yl)-acetamino)-7,8-dehydrorutaecarpine (**9i**)

The compound **8a** was reacted with excess *N*-methyl piperazine following the general procedure to give the desired product **9i** as a yellow solid in 74% yield. <sup>1</sup>H NMR (400 MHz, CDCl<sub>3</sub>): δ 9.86 (s, 1H), 9.46 (s, 1H), 8.74 (d, *J* = 7.6 Hz, 1H), 8.50 (d, *J* = 8.8 Hz, 1H), 8.28 (s, 1H), 8.04 (t, *J* = 7.7 Hz, 1H), 7.82 (d, *J* = 9.1 Hz, 1H), 7.60 – 7.46 (m, 3H), 7.37 – 7.29 (m, 1H), 3.21 (s, 2H), 2.71 (s, 4H), 2.57 (s, 4H), 2.37 (s, 3H); <sup>13</sup>C NMR (101 MHz, DMSO): δ 168.43, 158.28, 143.76, 139.79, 139.04, 135.25, 129.43, 127.62, 126.66, 126.35, 121.82, 120.66, 120.35, 119.26, 117.53, 115.97, 115.31, 112.66, 107.90, 61.78, 54.50, 52.67, 45.70. Purity: 96.6% by HPLC. HRMS (ESI): calcd for (M+H)<sup>+</sup> (C<sub>25</sub>H<sub>24</sub>N<sub>6</sub>O<sub>2</sub>) 441.2034, found 441.2022.

### 5.1.6.4 3-(2-Phenylamino-acetamino)-7,8-dehydrorutaecarpine (**9k**)

The compound **8a** was reacted with excess aniline following the general procedure to give the desired product **9k** as a yellow solid in 68% yield. <sup>1</sup>H NMR (400 MHz, DMSO): δ 12.70 (s, 1H), 10.42 (s, 1H), 8.74 (s, 1H), 8.70 – 8.57 (m, 1H), 8.19 (s, 1H), 8.11 (dd, *J* = 20.9, 6.3 Hz, 2H), 7.87 – 7.80 (m, 2H), 7.69 (d, *J* = 8.9 Hz, 1H), 7.50 (t, *J* = 7.1 Hz, 1H), 7.30 (t, *J* = 8.2 Hz, 1H), 7.12 (t, *J* = 7.2 Hz, 2H), 6.65 (d, *J* = 8.0 Hz, 1H), 6.59 (d, *J* = 7.0 Hz, 1H), 4.35 (d, *J* = 0.6 Hz, 1H), 4.03 – 3.88 (m, 2H); <sup>13</sup>C NMR (101 MHz, DMSO): δ 168.04, 158.28, 148.56, 143.68, 139.77, 139.03, 135.56, 129.42, 128.88, 127.14, 126.83, 126.35, 121.80, 120.65, 120.34, 119.24, 117.52, 116.02, 115.71, 114.90, 112.64, 112.08, 107.92, 40.71. Purity: 99.6% by HPLC. HRMS (ESI): calcd for (M-H)<sup>-</sup> (C<sub>26</sub>H<sub>19</sub>N<sub>5</sub>O<sub>2</sub>) 432.1466, found 432.1486.

### 5.1.6.5 3-(2-Dimethylamino-propionamino)-7,8-dehydrorutaecarpine (**10d**)

The compound **8b** was reacted with excess dimethylamine following the general procedure to give the desired product **10d** as a yellow solid in 63% yield. <sup>1</sup>H NMR (400 MHz, DMSO): δ 12.64 (s, 1H), 10.38 (s, 1H), 8.71

(s, 1H), 8.61 (d,  $J = 7.5$  Hz, 1H), 8.16 (d,  $J = 7.9$  Hz, 1H), 8.07 (d,  $J = 8.8$  Hz, 1H), 7.82 (t,  $J = 8.4$  Hz, 2H), 7.69 (d,  $J = 8.2$  Hz, 1H), 7.49 (t,  $J = 7.6$  Hz, 1H), 7.29 (t,  $J = 7.4$  Hz, 1H), 2.62 (t,  $J = 6.7$  Hz, 2H), 2.53 (d,  $J = 7.2$  Hz, 2H), 2.21 (s, 6H);  $^{13}\text{C}$  NMR (101 MHz, DMSO):  $\delta$  170.29, 158.29, 143.53, 139.79, 138.96, 135.94, 129.46, 127.20, 126.73, 126.30, 121.85, 120.62, 120.33, 119.18, 117.51, 116.05, 114.75, 112.65, 107.86, 55.03, 44.89, 34.79. Purity: 99.3% by HPLC. HRMS (ESI): calcd for  $(\text{M}+\text{H})^+$  ( $\text{C}_{23}\text{H}_{21}\text{N}_5\text{O}_2$ ) 400.1768, found 400.1765.

#### 5.1.6.6 3-(2-Diethylamino-propionamino)-7,8-dehydrorutaecarpine (**10e**)

The compound **8b** was reacted with excess diethylamine following the general procedure to give the desired product **10e** as a yellow solid in 69% yield.  $^1\text{H}$  NMR (400 MHz,  $\text{CDCl}_3$ ):  $\delta$  11.50 (s, 1H), 10.04 (s, 1H), 8.68 (t,  $J = 6.1$  Hz, 1H), 8.33 (s, 1H), 8.32 – 8.24 (m, 1H), 8.01 – 7.96 (m, 1H), 7.79 – 7.71 (m, 1H), 7.53 (d,  $J = 7.4$  Hz, 1H), 7.50 – 7.45 (m, 2H), 7.36 – 7.27 (m, 1H), 2.88 (m,  $J = 4.6$  Hz, 2H), 2.81 – 2.72 (t, 4H), 2.62 (m,  $J = 4.9$  Hz, 2H), 1.27 – 1.15 (m, 6H);  $^{13}\text{C}$  NMR (101 MHz, DMSO):  $\delta$  170.55, 158.33, 143.55, 139.80, 139.00, 135.98, 129.48, 127.23, 126.83, 126.37, 121.86, 120.70, 120.39, 119.22, 117.56, 116.10, 114.70, 112.66, 107.95, 48.30, 46.11, 34.17, 11.72. Purity: 98.0% by HPLC. HRMS (ESI): calcd for  $(\text{M}+\text{H})^+$  ( $\text{C}_{25}\text{H}_{25}\text{N}_5\text{O}_2$ ) 428.2081, found 428.2097.

#### 5.1.6.7 3-(2-N-Pyrrolyl-propionamino)-7,8-dehydrorutaecarpine (**10f**)

The compound **8b** was reacted with excess pyrrolidine following the general procedure to give the desired product **10f** as a yellow solid in 73% yield.  $^1\text{H}$  NMR (400 MHz, DMSO):  $\delta$  12.65 (s, 1H), 10.43 (s, 1H), 8.72 (d,  $J = 2.2$  Hz, 1H), 8.62 (d,  $J = 7.5$  Hz, 1H), 8.17 (d,  $J = 7.9$  Hz, 1H), 8.07 (dd,  $J = 8.9, 2.3$  Hz, 1H), 7.83 (dd,  $J = 8.2, 6.0$  Hz, 2H), 7.69 (d,  $J = 8.2$  Hz, 1H), 7.49 (t,  $J = 7.6$  Hz, 1H), 7.30 (t,  $J = 7.5$  Hz, 1H), 2.78 (t,  $J = 7.0$

Hz, 2H), 2.57 (t,  $J = 6.9$  Hz, 2H), 2.54 (t, 4H), 1.70 (m,  $J = 3.0$  Hz, 4H);  $^{13}\text{C}$  NMR (101 MHz, DMSO):  $\delta$  170.29, 158.32, 143.54, 139.79, 139.00, 135.97, 129.48, 127.23, 126.80, 126.36, 121.85, 120.69, 120.38, 119.21, 117.56, 116.08, 114.71, 112.66, 107.94, 53.38, 51.49, 36.14, 23.14. Purity: 98.7% by HPLC. HRMS (ESI): calcd for  $(\text{M}+\text{H})^+$  ( $\text{C}_{25}\text{H}_{23}\text{N}_5\text{O}_2$ ) 426.1925, found 426.1918.

#### 5.1.6.8 3-(2-*N*-Piperidyl-propionamino)-7,8-dehydrorutaecarpine (**10g**)

The compound **8b** was reacted with excess piperidine following the general procedure to give the desired product **10g** as a yellow solid in 77% yield.  $^1\text{H}$  NMR (400 MHz, DMSO):  $\delta$  12.65 (s, 1H), 10.51 (s, 1H), 8.71 (d,  $J = 1.8$  Hz, 1H), 8.62 (d,  $J = 7.5$  Hz, 1H), 8.17 (d,  $J = 7.9$  Hz, 1H), 8.06 (dd,  $J = 9.0, 2.2$  Hz, 1H), 7.83 (t,  $J = 8.2$  Hz, 2H), 7.69 (d,  $J = 8.1$  Hz, 1H), 7.49 (t,  $J = 7.6$  Hz, 1H), 7.30 (t,  $J = 7.5$  Hz, 1H), 2.69 – 2.63 (m, 2H), 2.54 (d,  $J = 6.7$  Hz, 2H), 2.42 (s, 4H), 1.58 – 1.48 (m, 4H), 1.45 – 1.35 (m, 2H);  $^{13}\text{C}$  NMR (101 MHz, DMSO):  $\delta$  170.45, 158.32, 143.54, 139.80, 139.00, 135.95, 129.48, 127.19, 126.84, 126.37, 121.86, 120.70, 120.38, 119.21, 117.55, 116.09, 114.66, 112.66, 107.95, 54.39, 53.63, 34.12, 25.61, 23.98. Purity: 99.7% by HPLC. HRMS (ESI): calcd for  $(\text{M}+\text{H})^+$  ( $\text{C}_{26}\text{H}_{25}\text{N}_5\text{O}_2$ ) 440.2081, found 440.2103.

#### 5.1.6.9 3-(2-*N*-Morpholinyl-propionamino)-7,8-dehydrorutaecarpine (**10h**)

The compound **8b** was reacted with excess morpholine following the general procedure to give the desired product **10h** as a yellow solid in 68% yield.  $^1\text{H}$  NMR (400 MHz, DMSO):  $\delta$  12.67 (s, 1H), 10.41 (s, 1H), 8.71 (d,  $J = 2.4$  Hz, 1H), 8.61 (d,  $J = 7.5$  Hz, 1H), 8.16 (d,  $J = 8.0$  Hz, 1H), 8.06 (dd,  $J = 9.0, 2.5$  Hz, 1H), 7.82 (dd,  $J = 8.2, 6.3$  Hz, 2H), 7.68 (d,  $J = 8.3$  Hz, 1H), 7.49 (t,  $J = 7.7$  Hz, 1H), 7.29 (t,  $J = 7.5$  Hz, 1H), 3.64 – 3.54 (t, 4H), 2.75 – 2.65 (t, 2H), 2.56 (t,  $J = 6.8$  Hz, 2H), 2.48 – 2.38 (t, 4H);  $^{13}\text{C}$  NMR (101 MHz, DMSO):  $\delta$  170.20, 158.31, 143.56, 139.79, 139.00, 135.90, 129.47, 127.22, 126.80, 126.35, 121.84, 120.68, 120.37, 119.21,

117.55, 116.07, 114.73, 112.66, 107.92, 66.18, 54.11, 53.01, 33.95. Purity: 99.3% by HPLC. HRMS (ESI): calcd for (M+H)<sup>+</sup> (C<sub>25</sub>H<sub>23</sub>N<sub>5</sub>O<sub>3</sub>) 442.1874, found 442.1872.

#### 5.1.6.10 3-(2-(4-Methylpiperazin-1-yl)-propionamino)-7,8-dehydrorutaecarpine (**10i**)

The compound **8b** was reacted with excess *N*-methyl piperazine following the general procedure to give the desired product **10i** as a yellow solid in 68% yield. <sup>1</sup>H NMR (400 MHz, DMSO<sub>3</sub>): δ 12.68 (s, 1H), 10.47 (s, 1H), 8.74 (d, *J* = 0.5 Hz, 1H), 8.62 (dd, *J* = 7.9, 3.0 Hz, 1H), 8.17 (d, *J* = 6.9 Hz, 1H), 8.08 (d, *J* = 8.4 Hz, 1H), 7.90 – 7.79 (m, 2H), 7.71 – 7.67 (m, 1H), 7.54 – 7.47 (m, 1H), 7.30 (t, *J* = 7.9 Hz, 1H), 4.00 – 3.90 (m, 2H), 3.60 – 3.47 (m, 4H), 3.23 – 3.10 (m, 4H), 2.97 – 2.87 (m, 2H), 1.23 (s, 3H); <sup>13</sup>C NMR (101 MHz, DMSO): δ 170.32, 158.35, 143.58, 139.81, 139.04, 135.95, 129.49, 127.25, 126.86, 126.40, 121.87, 120.73, 120.42, 119.25, 117.59, 116.10, 114.74, 112.68, 107.98, 58.81, 55.84, 55.24, 54.68, 53.64, 52.27, 51.76, 50.13, 47.09, 45.96, 45.60, 45.51, 41.41, 40.40, 39.93, 39.31, 39.00, 36.20, 34.17, 31.01. Purity: 99.7% by HPLC. HRMS (ESI): calcd for (M+H)<sup>+</sup> (C<sub>26</sub>H<sub>26</sub>N<sub>6</sub>O<sub>2</sub>) 445.2190, found 445.2199.

#### 5.1.6.11 3-(2-Phenylamino-propionamino)-7,8-dehydrorutaecarpine (**10k**)

The compound **8b** was reacted with excess aniline following the general procedure to give the desired product **10k** as a yellow solid in 71% yield. <sup>1</sup>H NMR (400 MHz, DMSO): δ 12.69 (s, 1H), 10.48 (s, 1H), 8.75 (s, 1H), 8.63 (d, *J* = 6.6 Hz, 1H), 8.17 (d, *J* = 7.6 Hz, 1H), 8.08 (d, *J* = 8.5 Hz, 1H), 7.85 (d, *J* = 7.8 Hz, 3H), 7.69 (d, *J* = 8.1 Hz, 1H), 7.49 (t, *J* = 8.3 Hz, 2H), 7.37 – 7.22 (m, 2H), 7.09 (d, *J* = 3.7 Hz, 1H), 6.59 (dd, *J* = 36.5, 6.0 Hz, 1H), 3.94 (d, *J* = 3.6 Hz, 2H), 3.48 – 3.36 (m, 1H), 2.98 – 2.85 (m, 2H); <sup>13</sup>C NMR (101 MHz, DMSO): δ 169.50, 164.76, 158.28, 148.10, 139.82, 135.56, 135.10, 129.28, 128.89, 127.48, 126.55, 121.79, 120.80, 120.46, 117.62, 116.58, 116.00, 115.34, 115.16, 112.68, 112.45, 108.08, 47.39, 43.54. Purity: 99.5% by

HPLC. HRMS (ESI): calcd for (M-H)<sup>-</sup> (C<sub>27</sub>H<sub>21</sub>N<sub>5</sub>O<sub>2</sub>) 446.1622, found 446.1589.

#### 5.1.6.12 3-(2-N-Pyrrolyl-butylamino)-7,8-dehydrorutaecarpine (**11f**)

The compound **8c** was reacted with excess pyrrolidine following the general procedure to give the desired product **11f** as a yellow solid in 67% yield. <sup>1</sup>H NMR (400 MHz, DMSO): δ 12.65 (s, 1H), 10.51 (s, 1H), 8.71 (d, *J* = 1.8 Hz, 1H), 8.62 (d, *J* = 7.5 Hz, 1H), 8.17 (d, *J* = 7.9 Hz, 1H), 8.06 (dd, *J* = 9.0, 2.2 Hz, 1H), 7.83 (t, *J* = 8.2 Hz, 2H), 7.69 (d, *J* = 8.1 Hz, 1H), 7.49 (t, *J* = 7.6 Hz, 1H), 7.30 (t, *J* = 7.5 Hz, 1H), 2.71 – 2.63 (m, 2H), 2.54 (d, *J* = 6.7 Hz, 2H), 2.42 (s, 4H), 1.61 – 1.49 (m, 4H), 1.42 (dd, *J* = 5.5, 5.1 Hz, 2H); <sup>13</sup>C NMR (101 MHz, DMSO): δ 170.44, 158.32, 143.54, 139.79, 138.99, 135.95, 129.48, 127.18, 126.84, 126.37, 121.85, 120.69, 120.38, 119.21, 117.55, 116.09, 114.66, 112.66, 107.95, 54.38, 53.63, 34.12, 25.61, 23.97. Purity: 99.4% by HPLC. HRMS (ESI): calcd for (M-H)<sup>-</sup> (C<sub>26</sub>H<sub>25</sub>N<sub>5</sub>O<sub>2</sub>) 438.1935, found 438.1931.

#### 5.1.7 General procedures for the preparation of compounds **10m** and **10n**

The suspension of compound **10d** or **10f** (0.25 mmol) in thiocyclopentane-1 with excess iodomethane (0.5 mL) was heated to 50 °C and gradually transformed to a clear solution. The precipitation was formed after stirring for 4h, cooled to 0 °C and washed with ether. The resulting crude product was purified by recrystallization from EtOH (15 mL) to afford **10m** and **10n**.

##### 5.1.7.1 3-(2-(*N,N,N*-Trimethyl)-propionamino)-7,8-dehydrorutaecarpine (**10m**)

The compound **10d** was treated with iodomethane following the general procedure to give the desired product **10m** as a yellow solid in 96% yield. <sup>1</sup>H NMR (400 MHz, DMSO): δ 12.69 (s, 1H), 10.59 (s, 1H), 8.73 (s, 1H), 8.62 (dd, *J* = 7.4, 3.0 Hz, 1H), 8.18 (d, *J* = 8.0 Hz, 1H), 8.06 (d, *J* = 8.8 Hz, 1H), 7.86 (t, *J* = 9.4 Hz, 2H), 7.70

(d,  $J = 8.1$  Hz, 1H), 7.50 (t,  $J = 7.5$  Hz, 1H), 7.31 (t,  $J = 7.4$  Hz, 1H), 3.73 (t,  $J = 7.2$  Hz, 2H), 3.14 (s, 9H), 3.04 – 2.96 (m, 2H);  $^{13}\text{C}$  NMR (101 MHz, DMSO):  $\delta$  167.27, 158.27, 143.82, 139.78, 139.09, 135.25, 129.39, 127.19, 126.93, 126.41, 121.78, 120.68, 120.37, 119.31, 117.49, 115.98, 115.08, 112.65, 108.00, 61.35, 52.50, 30.06. Purity: 98.9% by HPLC. HRMS (ESI): calcd for  $(\text{M})^+$  ( $\text{C}_{24}\text{H}_{24}\text{N}_5\text{O}_2$ ) 414.1925, found 414.1935.

#### 5.1.7.2 3-(2-(1-Methylpyrrolyl)-propionamino)-7,8-dehydrorutaecarpine (**10n**)

The compound **10f** was treated with iodomethane following the general procedure to give the desired product **10n** as a yellow solid in 90% yield.  $^1\text{H}$  NMR (400 MHz, DMSO):  $\delta$  12.69 (s, 1H), 10.59 (s, 1H), 8.73 (d,  $J = 2.2$  Hz, 1H), 8.66 – 8.58 (m, 1H), 8.23 – 8.15 (m, 1H), 8.06 (d,  $J = 8.4$  Hz, 1H), 7.86 (t,  $J = 8.6$  Hz, 1H), 7.69 (dd,  $J = 7.2, 3.4$  Hz, 1H), 7.55 – 7.45 (m, 1H), 7.30 (t,  $J = 7.1$  Hz, 1H), 3.79 – 3.68 (m, 2H), 3.61 – 3.46 (m, 4H), 3.06 (s, 3H), 3.02 – 2.97 (m, 2H), 2.13 (d,  $J = 2.1$  Hz, 4H);  $^{13}\text{C}$  NMR (101 MHz, DMSO):  $\delta$  167.46, 158.32, 143.85, 139.81, 139.14, 135.33, 129.43, 127.27, 126.99, 126.46, 121.81, 120.75, 120.43, 119.36, 117.55, 116.04, 115.10, 112.68, 108.07, 63.77, 59.01, 47.84, 30.76, 21.16. Purity: 95.5% by HPLC. HRMS (ESI): calcd for  $(\text{M})^+$  ( $\text{C}_{26}\text{H}_{26}\text{N}_5\text{O}_2$ ) 440.2081, found 440.2095.

#### 5.2 Inhibition studies on AChE and BuChE

Acetylcholinesterase (AChE, E.C. 3.1.1.7, from *electric eel*), butyrylcholinesterase (BuChE, E.C. 3.1.1.8, from *equine serum*), 5,5'-dithiobis-(2-nitrobenzoic acid) (Ellman's reagent, DTNB), acetylthiocholine chloride (ATC), butylthiocholine chloride (BTC), and tacrine hydrochloride were purchased from Sigma Aldrich.

All the assays were carried out in 0.1 M  $\text{KH}_2\text{PO}_4$  /  $\text{K}_2\text{HPO}_4$  buffer (pH 8.0). Enzyme solutions were prepared

by dissolving lyophilized powder in double-distilled water. Stock solutions of tested compounds (10 mM) were prepared in DMSO and diluted in phosphate buffer (pH 8.0). The assay solution (200  $\mu$ L) consist of phosphate buffer (pH 8.0), with the addition of 10  $\mu$ L of 0.01 M DTNB, 10  $\mu$ L of enzyme, and 10  $\mu$ L of 0.01 M substrate (ATC or BTC). Five increasing concentrations of inhibitors with their inhibitory activity ranged from 20% to 80% were added to the assay solution and pre-incubated for 15 min at 37 °C with the enzyme followed by the addition of corresponding substrate. Initial rate measurement assays were performed at 37 °C with a PowerWave XS2 microplate spectrophotometer. Absorbance value at 412 nm was recorded for 2 min, and the calculations were performed based on the method of Ellman *et al.* [38]. Each concentration was tested in triplicate, and IC<sub>50</sub> values were calculated graphically from log concentration-inhibition curve (Origin 7.5 software).

### 5.3 Kinetic characterization of AChE inhibition

Kinetic characterization of AChE inhibition was performed based on a reported method [34]. The assay solution (200  $\mu$ L) consist of 0.1 M phosphate buffer (pH 8.0), with the addition of 10  $\mu$ L of 0.01 M DTNB, 10  $\mu$ L of enzyme, and 10  $\mu$ L of substrate (ATC). Five different concentrations of inhibitors were added to the assay solution and pre-incubated for 15 min at 37 °C with the enzyme followed by the addition of substrate in different concentrations. Kinetic characterization for the hydrolysis of ATC catalyzed by AChE was carried out using spectrometric method at 412 nm. The parallel control experiments were performed without inhibitor in the assay.

### 5.4 Molecular docking

The crystal structure of AChE complexed with tacrine (code ID: 1ACJ) and BuChE complexed with

Echothiophate (code ID: 1POI) were obtained from the Protein Data Bank after eliminating the inhibitors and water molecules. The 3D Structure of **9b** was built, and its geometry optimization was performed with molecular mechanics. After addition of Gasteiger charges, removal of hydrogen atoms, addition of their atomic charges to skeleton atoms, and the assignment of proper atomic types, the further preparation of the inhibitor was accomplished. Autotors was then used to define the rotatable bonds in the ligands. Docking studies were performed using the AUTODOCK 4.0 program. By using ADT, polar hydrogen atoms were added to amino acid residues, and Gasteiger charges were assigned to all atoms of the enzyme. The resulting enzyme structure was used as an input for the AUTOGRID program. AUTOGRID performed a pre-calculated atomic affinity grid maps for each atom type in the ligand, plus an electrostatics map and a separate desolvation map presented in the substrate molecule. All maps were calculated with 0.375 Å spacing between grid points. The centre of the grid box was placed at the bottom of the active site gorge (AChE [2.781 64.383 67.971]; BuChE [112.0 20.0 40.0]). The dimensions of the active site box were set at 50 × 46 × 46 Å.

Flexible ligand docking was performed for the compounds. Docking calculations were carried out using the Lamarckian genetic algorithm (LGA), and all parameters were the same for each docking. After 100 docking runs, the procedure was ended and the obtained orientations were analyzed.

### *5.5 Determination of the inhibitory potency on self and AChE-induced A $\beta$ (1–42) aggregation*

Thioflavin T (ThT) assay was performed to determine the activities of our tested derivatives on inhibiting amyloid-beta (1–42) self-aggregation. A $\beta$ <sub>1–42</sub> peptide and tested compounds were dissolved in DMSO and diluted in 0.215 M sodium phosphate buffer (pH 8.0). The final concentration of A $\beta$ <sub>1–42</sub> and inhibitors were 50  $\mu$ M and 25  $\mu$ M. After incubating the peptide at 37 °C with and without the tested compounds for 48h, 180  $\mu$ L

of 5  $\mu\text{M}$  Thioflavin T (diluted in 50 mM glycine-NaOH buffer, pH 8.5) was added. Fluorescence intensity was carried out (excitation wavelength 450 nm, emission wavelength 485 nm) on a monochromators based multimode microplate reader (INFINITE M1000), and values at the plateau were averaged after subtraction of the background fluorescence of the 5  $\mu\text{M}$  Thioflavin T solution. The percent inhibition on self-aggregation was calculated with the following equation:  $(1 - I_{\text{Fi}}/I_{\text{Fc}}) \times 100\%$  where  $I_{\text{Fi}}$  and  $I_{\text{Fc}}$  were the fluorescence intensities obtained for absorbance in the presence and absence of inhibitors, respectively, minus the fluorescence of respective blanks. Each assay was run in triplicate and each reaction was repeated for at least three times.

For co-incubation experiment,  $\text{A}\beta_{1-42}$  peptide was lyophilized from 2 mg/mL HFIP (1,1,1,3,3,3-hexafluoro-2-propanol) and dissolved in DMSO. The mixtures containing 2  $\mu\text{L}$  of  $\text{A}\beta_{1-42}$  peptide and 16  $\mu\text{L}$  of AChE in the presence or absence of the tested compounds (2  $\mu\text{L}$ ) were incubated for 6h at 37  $^{\circ}\text{C}$ . The final volume of each vial was 20  $\mu\text{L}$  and the final concentrations of  $\text{A}\beta_{1-42}$  peptide (diluted in 0.215 M sodium phosphate buffer, pH 8.0) and AChE (dissolved in 0.1 M sodium phosphate buffer, pH 8.0) were 50  $\mu\text{M}$  and 0.5  $\mu\text{M}$ . Blanks containing  $\text{A}\beta_{1-42}$ , AChE,  $\text{A}\beta_{1-42}$  plus the tested compounds in 0.215 M sodium phosphate buffer were prepared. To analyze co-aggregation inhibition, the ThT fluorescence assay was used and measured at 450 nm (excitation wavelength) and 485 nm (emission wavelength) after adding 180  $\mu\text{L}$  of 5  $\mu\text{M}$  Thioflavin T (diluted in 50 mM glycine-NaOH buffer, pH 8.5) to the mixtures. The percent inhibition on AChE-induced aggregation was calculated with the following equation:  $(1 - I_{\text{Fi}}/I_{\text{Fc}}) \times 100\%$  where  $I_{\text{Fi}}$  and  $I_{\text{Fc}}$  were the fluorescence intensities obtained for  $\text{A}\beta_{1-42}$  plus AChE in the presence and absence of inhibitors, respectively, minus the fluorescence of respective blanks.

### 5.6 Measurement of the antioxidative activity

The antioxidative activity was determined based on the oxygen radical absorbance capacity-fluorescein (ORAC-FL) assay [44, 45]. The reaction was carried out in 75 mM potassium phosphate buffer (pH 7.4), and the final volume of reaction mixture was 200  $\mu\text{L}$ . The tested compounds and Trolox standard substance was dissolved in DMSO to 10 mM and diluted in 75 mM potassium phosphate buffer (pH 7.4). Antioxidant (20  $\mu\text{L}$ ) and fluorescein (FL, 120  $\mu\text{L}$ , final concentration of 140 nM) were incubated for 15 min at 37 °C placing in the wells of a black 96 well plate. Then 60  $\mu\text{L}$  of 2,2'-azobis(amidinopropane) dihydrochloride (AAPH, final concentration of 40 mM) solution was added rapidly. The fluorescence was recorded every minute for 240 min at 485 nm (excitation wavelength) and 535 nm (emission wavelength). The final concentration of tested compounds and Trolox standard substance was 1–5  $\mu\text{M}$ . A blank (FL + AAPH in 75 mM potassium phosphate buffer) instead of the sample and Trolox calibration solutions was used in each assay. All the reaction mixtures were carried out in triplicate, and each reaction was repeated for at least three times. Antioxidant curves (fluorescence versus time) were normalized to the curve of the blank in the same assay, and then the area under the fluorescence decay curve (AUC) was calculated. The net AUC of a sample was obtained by subtracting the AUC of the blank. ORAC-FL values were expressed as Trolox equivalents by using the standard curve calculated for each sample, where the ORAC-FL value of Trolox was taken as 1, indicating the antioxidative potency of the tested compounds.

### 5.7 Metal-chelating studies

The metal-chelating studies were carried out in a UV-vis spectrophotometer (SHIMADZC UV-2450PC). The UV absorption of the tested compound **9b**, in the absence or presence of NaCl, KCl,  $\text{MgCl}_2$ ,  $\text{CaCl}_2$ ,  $\text{CuSO}_4$ ,  $\text{FeSO}_4$ , and  $\text{ZnSO}_4$ , was recorded in a 1 cm quartz cuvette after incubating for 30 min at room temperature.

The final volume of reaction mixture was 1 mL, and the final concentrations of the tested compound **9b** and metals were 20  $\mu\text{M}$ . All the reaction mixtures were carried out in triplicate, and each reaction was repeated for at least three times.

The molar ratio method was performed to determine the stoichiometry of the complex **9b**-metal (II) by titrating the ethanol solution of compound **9b** with ascending amounts of  $\text{CuSO}_4$  [43]. The final concentration of the tested compound **9b** was 20  $\mu\text{M}$ , and the final concentration of  $\text{Cu}^+$  ranged from 1  $\mu\text{M}$  to 40  $\mu\text{M}$ . The UV spectra were recorded and treated by numerical subtraction of  $\text{CuSO}_4$  and **9b** at corresponding concentrations, plotted versus the mole fraction of **9b**.

#### *5.8 Cytotoxic effects on SH-SY5Y cells*

SH-SY5Y cells were maintained in Dulbecco's modified Eagle's medium (DMEM) and supplemented with 10% fetal calf serum, 100 U/mL penicillin, and 100 U/mL streptomycin. Cultures were maintained at 37 °C in 5%  $\text{CO}_2$ /air and were passaged twice weekly. For assays, SH-SY5Y cells were subcultured in 48-wells plates at a density of  $10^5$  cells per well for 24h, and treated with our lead compounds at 0.1, 1.0, 10, and 100  $\mu\text{M}$  for 48h. The cell viability was determined by using MTT colorimetry, measuring the absorption at 590 nm. Controls were taken as having 100% viability. Each concentration was tested in triplicate, and  $\text{IC}_{50}$  values were calculated graphically from log concentration-inhibition curve (Origin 7.5 software).

### **Acknowledgements**

We thank the Natural Science Foundation of China (Grants 81273433, 21172272), and the Specialized Research Fund for the Doctoral Program of Higher Education (20110171110051) for financial support of this study.

## References

- [1] D.M. Walsh, D.J. Selkoe, Deciphering the Molecular Basis of Memory Failure in Alzheimer's Disease, *Neuron*, 44 (2004) 181-193.
- [2] D.J. Selkoe, M.B. Podlisny, Deciphering the genetic basis of Alzheimer's disease, *Annu. Rev. Genomics Hum Genet*, 3 (2002) 67-99.
- [3] A.V. Terry, J.J. Buccafusco, The Cholinergic Hypothesis of Age and Alzheimer's Disease-Related Cognitive Deficits: Recent Challenges and Their Implications for Novel Drug Development, *J Pharmacol Exp Ther*, 306 (2003) 821-827.
- [4] G. Pacheco, R. Palacios-Esquivel, D.E. Moss, Cholinesterase inhibitors proposed for treating dementia in Alzheimer's disease: selectivity toward human brain acetylcholinesterase compared with butyrylcholinesterase, *J Pharmacol Exp Ther*, 274 (1995) 767-770.
- [5] D.R. Liston, J.A. Nielsen, A. Villalobos, D. Chapin, S.B. Jones, S.T. Hubbard, I.A. Shalaby, A. Ramirez, D. Nason, W.F. White, Pharmacology of selective acetylcholinesterase inhibitors: implications for use in Alzheimer's disease, *Euro J Pharmacol*, 486 (2004) 9-17.
- [6] D.E. Kuhl, R.A. Koeppe, S.E. Snyder, S. Minoshima, K.A. Frey, M.R. Kilbourn, In vivo butyrylcholinesterase activity is not increased in Alzheimer's disease synapses, *Ann Neurol*, 59 (2006) 13-20.
- [7] B.A. Yankner, L.R. Dawes, S. Fisher, L. Villa-Komaroff, M.L. Oster-Granite, R.L. Neve, Neurotoxicity of a fragment of the amyloid precursor associated with Alzheimer's disease, *Science*, 245 (1989) 417-420.

- [8] D.J. Selkoe, Translating cell biology into therapeutic advances in Alzheimer's disease, *Nature*, 399 (1999) A23-A31.
- [9] E.D. Thorsett, L.H. Latimer, Therapeutic approaches to Alzheimer's disease, *Curr Opin Chem Biol*, 4 (2000) 377-382.
- [10] G.P. Lim, T. Chu, F. Yang, W. Beech, S.A. Frautschy, G.M. Cole, The Curry Spice Curcumin Reduces Oxidative Damage and Amyloid Pathology in an Alzheimer Transgenic Mouse, *J Neurosci*, 21 (2001) 8370-8377.
- [11] Y.E. Kwon, J.Y. Park, K.T. No, J.H. Shin, S.K. Lee, J.S. Eun, J.H. Yang, T.Y. Shin, D.K. Kim, B.S. Chae, J.Y. Leem, K.H. Kim, Synthesis, in vitro assay, and molecular modeling of new piperidine derivatives having dual inhibitory potency against acetylcholinesterase and A $\beta$ 1-42 aggregation for Alzheimer's disease therapeutics, *Bioorg Med Chem*, 15 (2007) 6596-6607.
- [12] G. Colombo, I. Daidone, E. Gazit, A. Amadei, A. Di Nola, Molecular dynamics simulation of the aggregation of the core-recognition motif of the islet amyloid polypeptide in explicit water, *Proteins*, 59 (2005) 519-527.
- [13] G.G. Tartaglia, A. Cavalli, R. Pellarin, A. Caflisch, The role of aromaticity, exposed surface, and dipole moment in determining protein aggregation rates, *Protein Sci*, 13 (2004) 1939-1941.
- [14] S. Verma, A. Singh, A. Mishra, The effect of fulvic acid on pre- and postaggregation state of A $\beta$ (17-42): Molecular dynamics simulation studies, *Biochim Biophys Acta*, (2012).
- [15] Y. Porat, A. Abramowitz, E. Gazit, Inhibition of Amyloid Fibril Formation by Polyphenols: Structural Similarity and Aromatic Interactions as a Common Inhibition Mechanism, *Chem Biol Drug Des*, 67 (2006) 27-37.
- [16] R. Scherzer-Attali, R. Pellarin, M. Convertino, A. Frydman-Marom, N. Egoz-Matia, S. Peled, M. Levy-Sakin, D.E. Shalev, A. Caflisch, E. Gazit, D. Segal, Complete Phenotypic Recovery of an Alzheimer's Disease Model by a Quinone-Tryptophan Hybrid Aggregation Inhibitor, *PLoS ONE*, 5 (2010) e11101.
- [17] T.J. Gibson, R.M. Murphy, Design of Peptidyl Compounds That Affect  $\beta$ -Amyloid Aggregation: Importance of

- Surface Tension and Context†, *Biochem*, 44 (2005) 8898-8907.
- [18] J.M. Mason, N. Kokkoni, K. Stott, A.J. Doig, Design strategies for anti-amyloid agents, *Curr Opin Stru Biol*, 13 (2003) 526-532.
- [19] E. Brandenburg, H. von Berlepsch, U.I.M. Gerling, C. Böttcher, B. Koksche, Inhibition of Amyloid Aggregation by Formation of Helical Assemblies, *Chem Euro J*, 17 (2011) 10651-10661.
- [20] M.L. Bolognesi, A. Cavalli, C. Melchiorre, Memoquin: A Multi-Target-Directed Ligand as an Innovative Therapeutic Opportunity for Alzheimer's Disease, *Neurotherapeutics*, 6 (2009) 152-162.
- [21] M.L. Bolognesi, V. Andrisano, M. Bartolini, R. Banzi, C. Melchiorre, Propidium-Based Polyamine Ligands as Potent Inhibitors of Acetylcholinesterase and Acetylcholinesterase-Induced Amyloid- $\beta$  Aggregation, *J Med Chem*, 48 (2004) 24-27.
- [22] N.C. Inestrosa, A. Alvarez, C.A. Pérez, R.D. Moreno, M. Vicente, C. Linker, O.I. Casanueva, C. Soto, J. Garrido, Acetylcholinesterase Accelerates Assembly of Amyloid-2-Peptides into Alzheimer's Fibrils: Possible Role of the Peripheral Site of the Enzyme, *Neuron*, 16 (1996) 881-891.
- [23] M. Rosini, E. Simoni, M. Bartolini, A. Cavalli, L. Ceccarini, N. Pascu, D.W. McClymont, A. Tarozzi, M.L. Bolognesi, A. Minarini, V. Tumiatti, V. Andrisano, I.R. Mellor, C. Melchiorre, Inhibition of Acetylcholinesterase,  $\beta$ -Amyloid Aggregation, and NMDA Receptors in Alzheimer's Disease: A Promising Direction for the Multi-target-Directed Ligands Gold Rush, *J Med Chem*, 51 (2008) 4381-4384.
- [24] P. Camps, X. Formosa, C. Galdeano, T.n. Gómez, D. Muñoz-Torrero, M. Scarpellini, E. Viayna, A. Badia, M.V.r. Clos, A. Camins, M. Pallàs, M. Bartolini, F. Mancini, V. Andrisano, J. Estelrich, M.n. Lizondo, A. Bidon-Chanal, F.J. Luque, Novel Donepezil-Based Inhibitors of Acetyl- and Butyrylcholinesterase and Acetylcholinesterase-Induced  $\beta$ -Amyloid Aggregation, *J Med Chem*, 51 (2008) 3588-3598.
- [25] M.A. Ansari, S.W. Scheff, Oxidative stress in the progression of Alzheimer disease in the frontal cortex, *J*

- Neuropathol Exp Neurol, 69 (2010) 155-167.
- [26] V.P. Reddy, X. Zhu, G. Perry, M.A. Smith, Oxidative stress in diabetes and Alzheimer's disease, *J Alzheimer's Dis: JAD*, 16 (2009) 763-774.
- [27] F. Gu, M. Zhu, J. Shi, Y. Hu, Z. Zhao, Enhanced oxidative stress is an early event during development of Alzheimer-like pathologies in presenilin conditional knock-out mice, *Neurosci Lett*, 440 (2008) 44-48.
- [28] X. Huang, R.D. Moir, R.E. Tanzi, A.I. Bush, J.T. Rogers, Redox-Active Metals, Oxidative Stress, and Alzheimer's Disease Pathology, *Ann N Y Acad Sci*, 1012 (2004) 153-163.
- [29] D.R.C. McLachlan, T.P.A. Kruck, W. Kalow, D.F. Andrews, A.J. Dalton, M.Y. Bell, W.L. Smith, Intramuscular desferrioxamine in patients with Alzheimer's disease, *Lancet*, 337 (1991) 1304-1308.
- [30] B.A.I.M.A. Ritchie Cw, et al., Metal-protein attenuation with iodochlorhydroxyquin (clioquinol) targeting  $\text{A}\beta$  amyloid deposition and toxicity in alzheimer disease: A pilot phase 2 clinical trial, *Arch Neurol*, 60 (2003) 1685-1691.
- [31] L. Lannfelt, K. Blennow, H. Zetterberg, S. Batsman, D. Ames, J. Harrison, C.L. Masters, S. Targum, A.I. Bush, R. Murdoch, J. Wilson, C.W. Ritchie, Safety, efficacy, and biomarker findings of PBT2 in targeting  $\text{A}\beta$  as a modifying therapy for Alzheimer's disease: a phase IIa, double-blind, randomised, placebo-controlled trial, *Lancet Neurol*, 7 (2008) 779-786.
- [32] A.I. Bush, Drug Development Based on the Metals Hypothesis of Alzheimer's Disease, *J Alzheimer's Dis*, 15 (2008) 223-240.
- [33] A. Cavalli, M.L. Bolognesi, A. Minarini, M. Rosini, V. Tumiatti, M. Recanatini, C. Melchiorre, Multi-target-directed ligands to combat neurodegenerative diseases, *J Med Chem*, 51 (2008) 347-372.
- [34] B. Wang, Y.-C. Mai, Y. Li, J.-Q. Hou, S.-L. Huang, T.-M. Ou, J.-H. Tan, L.-K. An, D. Li, L.-Q. Gu, Z.-S. Huang, Synthesis and evaluation of novel rutaecarpine derivatives and related alkaloids derivatives as selective

- acetylcholinesterase inhibitors, *Euro J Med Chem*, 45 (2010) 1415-1423.
- [35] W. Yang, Y. Wong, O.T.W. Ng, L.-P. Bai, D.W.J. Kwong, Y. Ke, Z.-H. Jiang, H.-W. Li, K.K.L. Yung, M.S. Wong, Inhibition of Beta-Amyloid Peptide Aggregation by Multifunctional Carbazole-Based Fluorophores, *Angew Chem Int Ed*, 51 (2012) 1804-1810.
- [36] Y.-Z. Tang, Z.-Q. Liu, Free-radical-scavenging effect of carbazole derivatives on AAPH-induced hemolysis of human erythrocytes, *Bioorg Med Chem*, 15 (2007) 1903-1913.
- [37] J. Bergman, S. Bergman, Studies of rutaecarpine and related quinazolinocarboline alkaloids, *J Org Chem*, 50 (1985) 1246-1255.
- [38] G.L. Ellman, K.D. Courtney, V. Andres, Jr., R.M. Feather-Stone, A new and rapid colorimetric determination of acetylcholinesterase activity, *Biochem pharmacol*, 7 (1961) 88-95.
- [39] G.M. Morris, D.S. Goodsell, R.S. Halliday, R. Huey, W.E. Hart, R.K. Belew, A.J. Olson, Automated docking using a Lamarckian genetic algorithm and an empirical binding free energy function, *J Comput Chem*, 19 (1998) 1639-1662.
- [40] P. Deb, A. Sharma, P. Piplani, R. Akkinepally, Molecular docking and receptor-specific 3D-QSAR studies of acetylcholinesterase inhibitors, *Mol Divers*, 16 (2012) 803-823.
- [41] M. Bartolini, C. Bertucci, M.L. Bolognesi, A. Cavalli, C. Melchiorre, V. Andrisano, Insight Into the Kinetic of Amyloid  $\beta$  (1–42) Peptide Self-Aggregation: Elucidation of Inhibitors' Mechanism of Action, *ChemBioChem*, 8 (2007) 2152-2161.
- [42] P. Kapková, V. Alptüzün, P. Frey, E. Erciyas, U. Holzgrabe, Search for dual function inhibitors for Alzheimer's disease: Synthesis and biological activity of acetylcholinesterase inhibitors of pyridinium-type and their A $\beta$  fibril formation inhibition capacity, *Bioorg Med Chem*, 14 (2006) 472-478.
- [43] M.L. Bolognesi, A. Cavalli, L. Valgimigli, M. Bartolini, M. Rosini, V. Andrisano, M. Recanatini, C. Melchiorre,

Multi-Target-Directed Drug Design Strategy: From a Dual Binding Site Acetylcholinesterase Inhibitor to a Trifunctional Compound against Alzheimer's Disease, *J Med Chem*, 50 (2007) 6446-6449.

[44] B. Ou, M. Hampsch-Woodill, R.L. Prior, Development and Validation of an Improved Oxygen Radical Absorbance Capacity Assay Using Fluorescein as the Fluorescent Probe, *J Agric Food Chem*, 49 (2001) 4619-4626.

[45] A. Dávalos, C. Gómez-Cordovés, B. Bartolomé, Extending Applicability of the Oxygen Radical Absorbance Capacity (ORAC–Fluorescein) Assay, *J Agric Food Chem*, 52 (2003) 48-54.

## Figure and Scheme Captions

**Figure 1.** Structures of rutaecarpine (**Ru**), 7,8-dehydrorutaecarpine (**DHRu**), and **DHRu** derivatives.

**Figure 2.** The Lineweaver-Burk plots for the inhibition of acetylcholinesterase by compounds **9b** (A) and **10f** (B). The lineweaver-Burk reciprocal plots of initial velocity and substrates concentrations were presented. Lines were derived from a weighted least-square analysis of the data points.

**Figure 3.** Docking models of compound-enzyme complex. Compound **9b** interacts with residues in the binding sites of *TcAChE* (A) and *HuBuChE* (B). The compound was rendered in yellow sticks, and the residues were rendered in pink sticks. Pictures were generated with Discovery Studio 2.5.

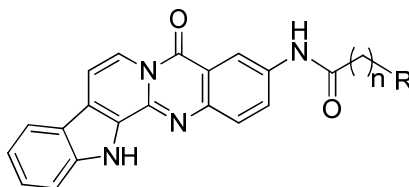
**Figure 4.** The inhibition of self (A) and AChE-induced (B)  $A\beta_{1-42}$  aggregation by the tested compounds at concentration of 25  $\mu\text{M}$ .  $A\beta_{1-42}$  was mixed with the compounds, and the aliquots were kept at 37  $^{\circ}\text{C}$  for 48h (A) or 6h (B). Buffer: 0.215 M sodium phosphate buffer, pH 8.0. Cur: curcumin; Tac: tacrine; PI: propidium iodide; CR: Congo-red.

**Figure 5.** (A) The UV spectrum of compound **9b** (20  $\mu\text{M}$ ) alone or in the presence of NaCl, KCl,  $\text{MgCl}_2$ ,  $\text{CaCl}_2$ ,  $\text{CuSO}_4$ ,  $\text{ZnSO}_4$ , and  $\text{FeSO}_4$  (20  $\mu\text{M}$ ). (B) Determination of the stoichiometry of complex **9b**-Cu (II) by using molar ratio method through titrating the ethanol solution of compound **9b** with ascending amounts of  $\text{CuSO}_4$ . The final concentration of the tested compound **9b** was 20  $\mu\text{M}$ , and the final concentration of  $\text{Cu}^+$  ranged from 1  $\mu\text{M}$  to 40  $\mu\text{M}$ .

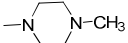
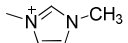
**Scheme 1.** Synthetic pathway for 3-aminoalkanamido-substituted 7,8-dehydrorutaecarpine derivatives.

Reagents and conditions: (i) ClCO(CH<sub>2</sub>)<sub>n</sub>Cl, CH<sub>2</sub>Cl<sub>2</sub>, K<sub>2</sub>CO<sub>3</sub>, reflux; (ii) DDQ, Dioxane, DMSO, reflux; (iii) for **9d–9i**, **9k**, **10d–10i**, **10k** and **11f**: the appropriate secondary amine, EtOH, KI, reflux; for **9a–9c**, **9j**, **10a–10c**, **10j**, **11a** and **11c**: the appropriate *N*-heterocyclic amine, reflux; (iv) for **10m** and **10n**: CH<sub>3</sub>I, thiocyclopentane-1, 50 °C; (v) the appropriate aromatic acid, EDCI, DIPEA, THF, room temperature.

**Scheme 2.** Synthesis of 3-amino-rutaecarpine (**6**) [23]. Reagents and conditions: (i) (CF<sub>3</sub>CO)<sub>2</sub>O, pyridine, room temperature; (ii) tryptamine, reflux; (iii) HCl, AcOH, reflux; (iv) 10% Pd/C, H<sub>2</sub>, MeOH, reflux; (v) KOH, H<sub>2</sub>O, EtOH, reflux.

**Table 1.** Inhibition of AChE and BuChE by target compounds, and their selectivity index

Compound	n	R	IC <sub>50</sub> <sup>a</sup> for AChE (nM)	IC <sub>50</sub> <sup>b</sup> for BuChE (nM)	Selectivity index <sup>c</sup>
<b>9a</b>	1		0.8 ± 0.2	2451 ± 10	3225
<b>9b</b>	1		0.6 ± 0.7	1855 ± 11	3092
<b>9c</b>	1		8.0 ± 0.3	7340 ± 30	922
<b>9d</b>	1	-N(CH <sub>3</sub> ) <sub>2</sub>	70.1 ± 0.3	26500 ± 150	378
<b>9e</b>	1	-N(CH <sub>2</sub> CH <sub>3</sub> ) <sub>2</sub>	70.4 ± 0.5	24100 ± 130	342
<b>9f</b>	1		59.3 ± 0.9	14400 ± 100	243
<b>9g</b>	1		70.0 ± 1.2	23200 ± 130	331
<b>9h</b>	1		87.8 ± 0.9	28500 ± 120	325
<b>9i</b>	1		158.0 ± 1.0	29100 ± 160	184
<b>9j</b>	1		3.09 ± 0.4	7300 ± 40	2362
<b>9k</b>	1		77.9 ± 0.8	25300 ± 120	325
<b>9l</b>	1		116.1 ± 0.9	24900 ± 100	214
<b>10a</b>	2		2.3 ± 0.5	4291 ± 20	1858
<b>10b</b>	2		2.1 ± 0.3	3488 ± 25	1638
<b>10c</b>	2		9.3 ± 0.7	7019 ± 37	756
<b>10d</b>	2	-N(CH <sub>3</sub> ) <sub>2</sub>	56.1 ± 1.0	21400 ± 160	382
<b>10e</b>	2	-N(CH <sub>2</sub> CH <sub>3</sub> ) <sub>2</sub>	64.1 ± 0.4	28300 ± 180	442

<b>10f</b>	2		13.9 ± 0.1	14900 ± 120	1072
<b>10g</b>	2		51.0 ± 0.7	24000 ± 160	471
<b>10h</b>	2		78.6 ± 1.4	27600 ± 170	351
<b>10i</b>	2		141.0 ± 2.0	28900 ± 130	205
<b>10j</b>	2		14.3 ± 0.4	6430 ± 33	450
<b>10k</b>	2		87.5 ± 1.2	27800 ± 110	318
<b>10l</b>	2		108.4 ± 0.7	26100 ± 100	241
<b>10m</b>	2		197.0 ± 1.0	37200 ± 240	189
<b>10n</b>	2		137.0 ± 2.0	17100 ± 120	125
<b>11a</b>	3		3.9 ± 0.2	4160 ± 31	1056
<b>11c</b>	3		11.7 ± 0.5	8200 ± 43	701
<b>11f</b>	3		84.6 ± 0.9	18500 ± 100	219
<b>11l</b>	3		136 ± 1.1	24600 ± 100	180
Tacrine	–	–	108.0 ± 2.0	33.4 ± 0.7	0.3

<sup>a</sup> AChE from *electric eel*; IC<sub>50</sub>, inhibitor concentration (means ± SEM for these experiments) resulting in 50% inhibition of AChE.

<sup>b</sup> BuChE from *equine serum*; IC<sub>50</sub>, inhibitor concentration (means ± SEM for these experiments) resulting in 50% inhibition of BuChE.

<sup>c</sup> Selectivity index = IC<sub>50</sub> (BuChE)/IC<sub>50</sub> (AChE).

**Table 2.** Inhibition of self and AChE-induced A $\beta_{1-42}$  aggregation, ORAC values and cytotoxic effects on SH-SY5Y

Compound	A $\beta_{1-42}$ aggregation inhibition <sup>a</sup> (%)	Inhibition of AChE-induced A $\beta_{1-42}$ aggregation <sup>b</sup> (%)	ORAC <sup>c</sup>		IC <sub>50</sub> for SH-SY5Y cytotoxic <sup>d</sup> ( $\mu$ M)
			5 $\mu$ M	1 $\mu$ M	
<b>9a</b>	43.7 $\pm$ 3.9	92.8 $\pm$ 0.9	1.8 $\pm$ 0.2	1.5 $\pm$ 0.1	>100
<b>9b</b>	45.9 $\pm$ 2.5	90.6 $\pm$ 1.3	2.3 $\pm$ 0.2	1.8 $\pm$ 0.2	>100
<b>9c</b>	51.4 $\pm$ 1.4	90.0 $\pm$ 1.7	2.0 $\pm$ 0.2	2.0 $\pm$ 0.1	>100
<b>9d</b>	47.0 $\pm$ 2.5	78.7 $\pm$ 1.9	3.2 $\pm$ 0.1	2.6 $\pm$ 0.2	4.1 $\pm$ 0.3
<b>9e</b>	36.9 $\pm$ 2.9	77.2 $\pm$ 3.5	2.7 $\pm$ 0.2	2.2 $\pm$ 0.2	2.3 $\pm$ 0.2
<b>9f</b>	35.3 $\pm$ 1.6	80.4 $\pm$ 3.3	2.4 $\pm$ 0.2	1.8 $\pm$ 0.2	2.9 $\pm$ 0.2
<b>9g</b>	38.9 $\pm$ 1.9	79.3 $\pm$ 2.9	2.3 $\pm$ 0.2	2.2 $\pm$ 0.1	6.3 $\pm$ 0.5
<b>9h</b>	12.1 $\pm$ 1.6	78.4 $\pm$ 3.7	2.0 $\pm$ 0.1	1.6 $\pm$ 0.1	9.9 $\pm$ 0.8
<b>9i</b>	49.5 $\pm$ 1.9	76.7 $\pm$ 2.5	3.4 $\pm$ 0.1	3.1 $\pm$ 0.1	8.6 $\pm$ 0.6
<b>9j</b>	43.9 $\pm$ 1.2	87.9 $\pm$ 2.6	n.d. <sup>e</sup>	n.d. <sup>e</sup>	n.d. <sup>e</sup>
<b>9k</b>	25.3 $\pm$ 0.8	78.6 $\pm$ 2.3	n.d. <sup>e</sup>	n.d. <sup>e</sup>	n.d. <sup>e</sup>
<b>9l</b>	42.4 $\pm$ 1.3	76.8 $\pm$ 2.2	n.d. <sup>e</sup>	n.d. <sup>e</sup>	n.d. <sup>e</sup>
<b>10a</b>	61.4 $\pm$ 1.9	90.3 $\pm$ 3.4	2.5 $\pm$ 0.1	2.3 $\pm$ 0.2	>100
<b>10b</b>	53.7 $\pm$ 2.5	89.6 $\pm$ 3.2	2.3 $\pm$ 0.2	1.8 $\pm$ 0.2	>100
<b>10c</b>	44.9 $\pm$ 2.1	87.0 $\pm$ 2.9	2.4 $\pm$ 0.2	2.1 $\pm$ 0.2	>100
<b>10d</b>	51.8 $\pm$ 0.9	77.9 $\pm$ 3.0	3.9 $\pm$ 0.1	3.0 $\pm$ 0.1	5.5 $\pm$ 0.4
<b>10e</b>	49.3 $\pm$ 2.5	77.3 $\pm$ 2.2	3.6 $\pm$ 0.2	2.6 $\pm$ 0.2	12.4 $\pm$ 1.0
<b>10f</b>	50.0 $\pm$ 2.1	81.4 $\pm$ 2.1	3.3 $\pm$ 0.2	3.0 $\pm$ 0.1	21.2 $\pm$ 1.6
<b>10g</b>	41.2 $\pm$ 1.6	83.0 $\pm$ 3.9	2.5 $\pm$ 0.2	1.9 $\pm$ 0.2	5.0 $\pm$ 0.4
<b>10h</b>	19.9 $\pm$ 1.2	76.7 $\pm$ 3.0	2.1 $\pm$ 0.1	2.0 $\pm$ 0.2	3.1 $\pm$ 0.3

<b>10i</b>	49.7 ± 1.1	77.3 ± 2.1	3.0 ± 0.1	2.5 ± 0.1	13.3 ± 1.2
<b>10j</b>	48.7 ± 1.6	84.3 ± 2.9	n.d. <sup>e</sup>	n.d. <sup>e</sup>	n.d. <sup>e</sup>
<b>10k</b>	20.6 ± 1.3	76.9 ± 2.5	n.d. <sup>e</sup>	n.d. <sup>e</sup>	n.d. <sup>e</sup>
<b>10l</b>	47.1 ± 1.4	78.8 ± 2.6	n.d. <sup>e</sup>	n.d. <sup>e</sup>	n.d. <sup>e</sup>
<b>10m</b>	38.3 ± 2.5	82.1 ± 1.9	1.9 ± 0.2	1.9 ± 0.1	29.2 ± 2.1
<b>10n</b>	44.9 ± 2.1	83.9 ± 1.6	2.0 ± 0.1	1.7 ± 0.2	19.1 ± 2.0
<b>11a</b>	60.3 ± 1.8	90.1 ± 1.5	n.d. <sup>e</sup>	n.d. <sup>e</sup>	n.d. <sup>e</sup>
<b>11c</b>	55.1 ± 1.6	88.4 ± 1.3	n.d. <sup>e</sup>	n.d. <sup>e</sup>	n.d. <sup>e</sup>
<b>11f</b>	45.6 ± 1.3	80.1 ± 2.0	n.d. <sup>e</sup>	n.d. <sup>e</sup>	n.d. <sup>e</sup>
<b>11l</b>	49.2 ± 1.3	75.9 ± 1.2	n.d. <sup>e</sup>	n.d. <sup>e</sup>	n.d. <sup>e</sup>
Curcumin	50.2 ± 2.2	35.1 ± 2.9	2.8 ± 0.2	2.5 ± 0.2	35.6 ± 3.1
Tacrine	n.d. <sup>e</sup>	5.0 ± 3.3	n.d. <sup>e</sup>	n.d. <sup>e</sup>	n.d. <sup>e</sup>
Propidium Iodide	n.d. <sup>e</sup>	84.5 ± 3.9	n.d. <sup>e</sup>	n.d. <sup>e</sup>	n.d. <sup>e</sup>
Congo-Red	n.d. <sup>e</sup>	95.4 ± 3.8	n.d. <sup>e</sup>	n.d. <sup>e</sup>	n.d. <sup>e</sup>

<sup>a</sup> The Thioflavin-T fluorescence method was used. The maximum percentage inhibitions of aggregation (means ± SEM for these experiments) were found at the inhibitors' concentration of 25 μM.

<sup>b</sup> Co-aggregation inhibition of Aβ<sub>1-42</sub> and AChE (0.5 μM) was detected by ThT assay. The maximum percentage inhibitions of aggregation (means ± SEM for these experiments) were found at the inhibitors' concentration of 25 μM.

<sup>c</sup> Data were expressed as μmol of Trolox equivalents/μmol of tested compounds. The concentration of the tested compounds was 5 μM and 1 μM.

<sup>d</sup> MTT method was carried out in the presence of 0.1, 1, 10, and 100 μM of compounds. IC<sub>50</sub>, the tested compounds' concentration (means ± SEM for these experiments) resulting in 50% mortality of SH-SY5Y.

<sup>e</sup> Not determined.

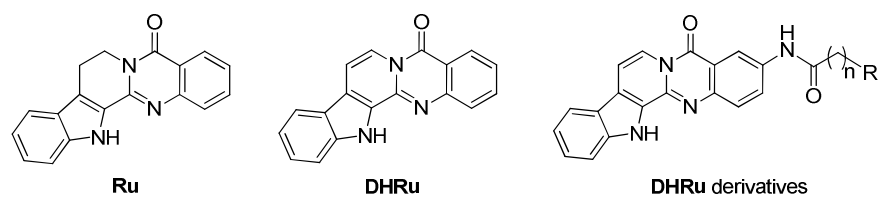


Figure 1

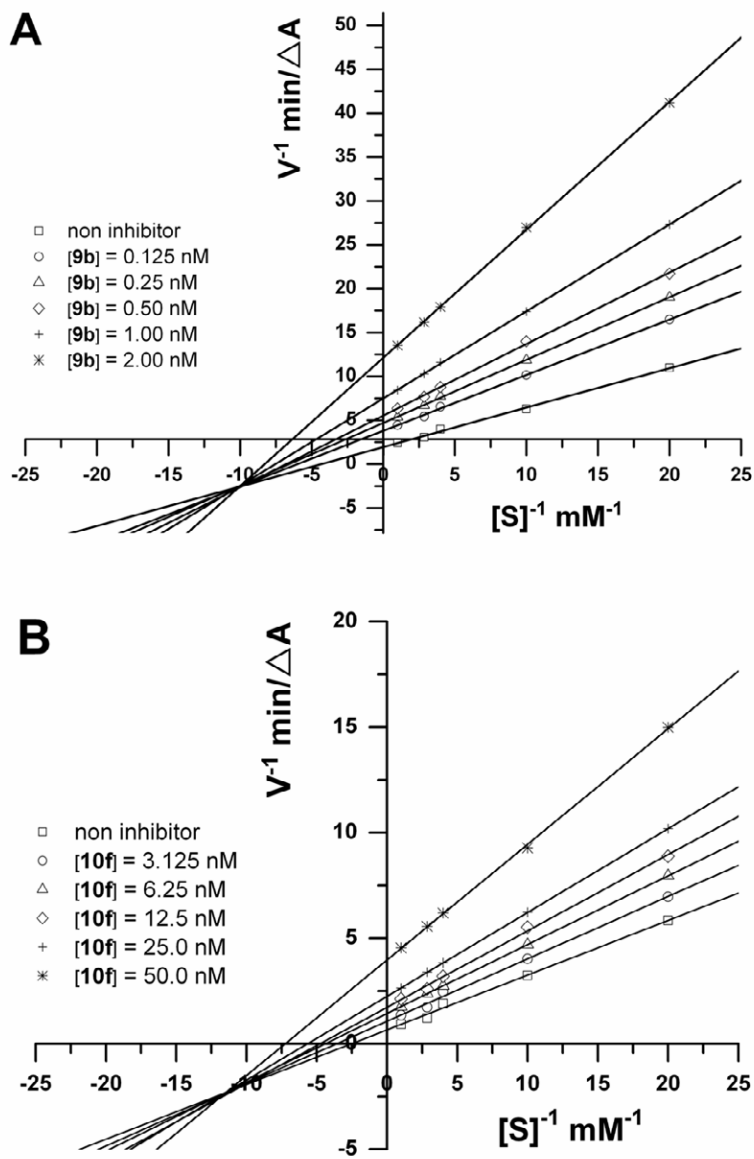


Figure 2

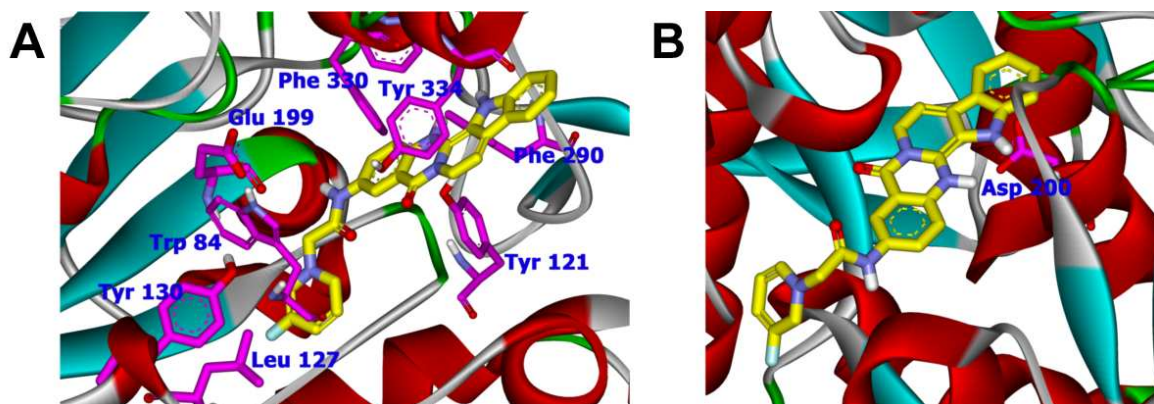


Figure 3

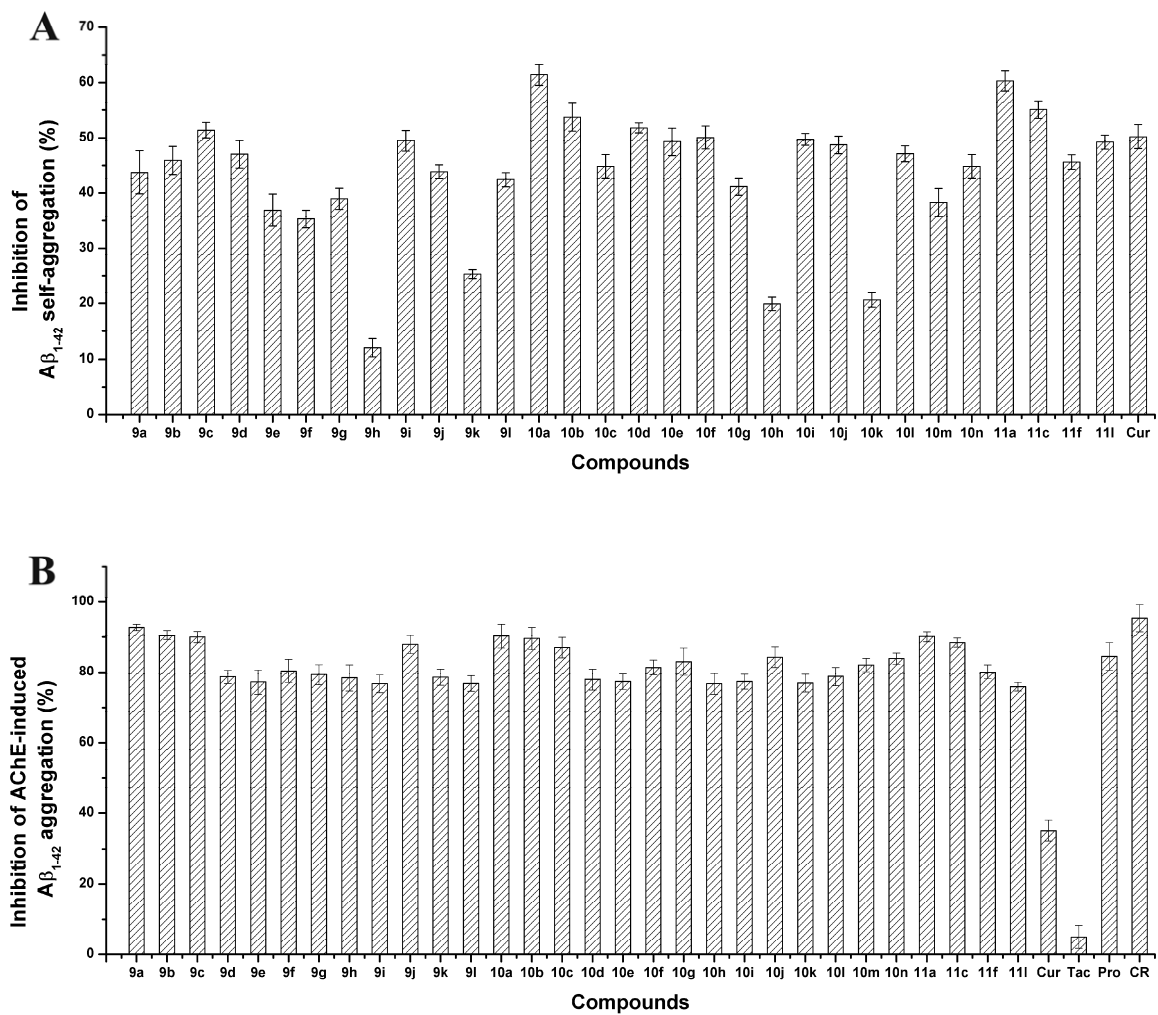


Figure 4

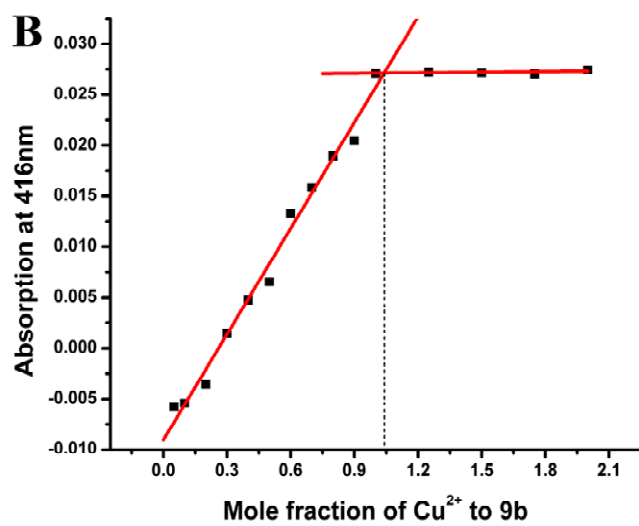
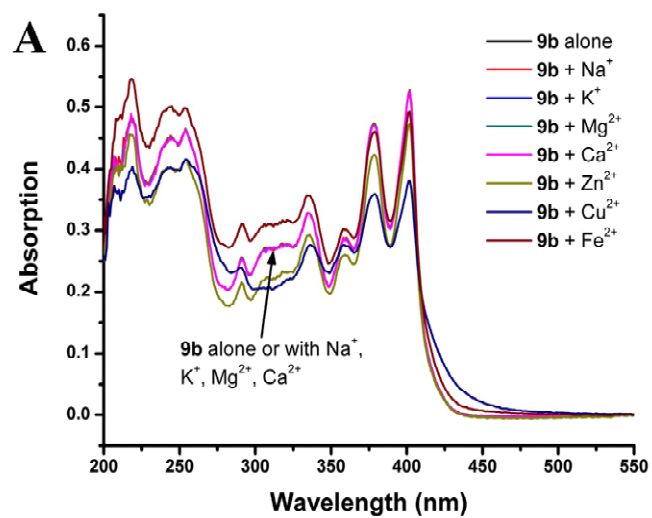
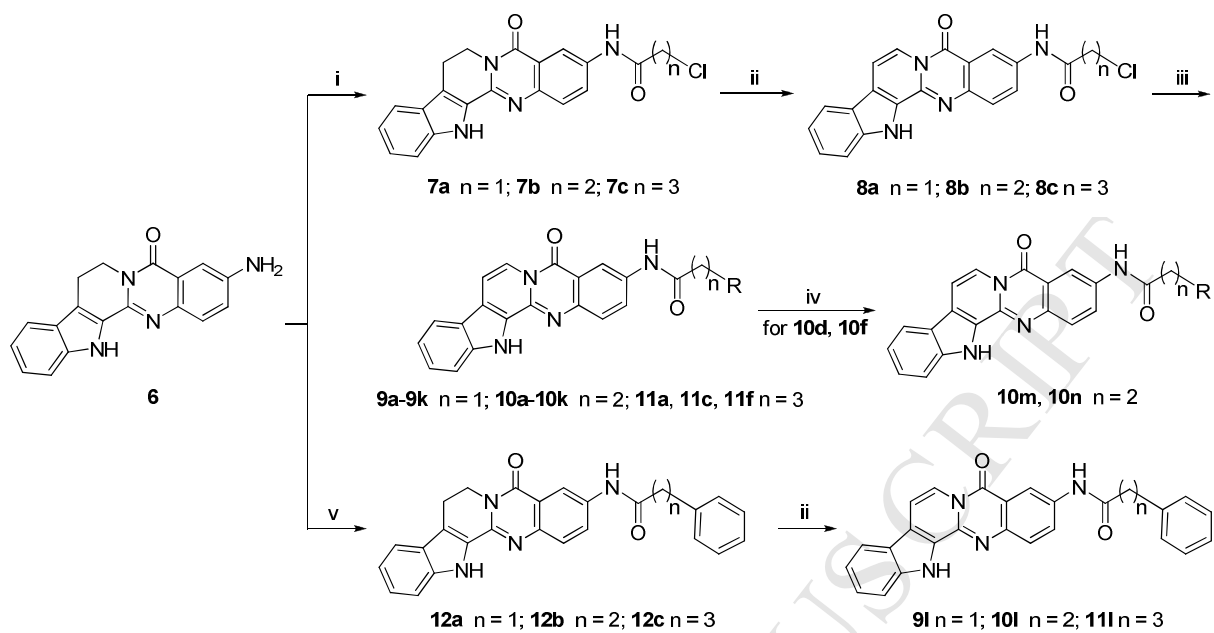
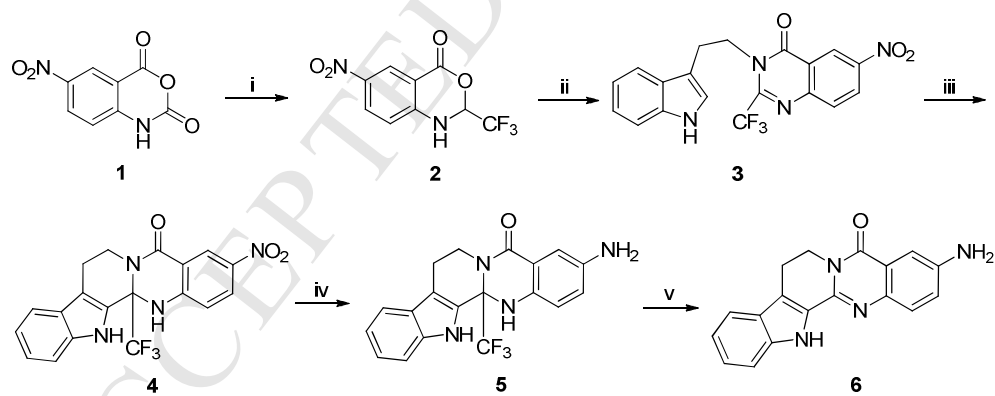


Figure 5



Scheme 1



Scheme 2

**Research highlights**

- ▶ 3-aminoalkanamido-substituted 7,8-dehydrorutaecarpine derivatives were synthesized.
- ▶ Compounds showed high inhibitory potencies and selectivity for AChE.
- ▶ Compounds had high activities inhibiting AChE-induced A $\beta$  aggregation.
- ▶ Compounds could act as antioxidants and metal chelators.